n draft biomass gasification using CFD

Abstract

Biomass gasifier is a device that converts solid biomass (ex. Wood, agro residues like wheat straw, mustered straw etc) into a combustible gas called as producer gas. The composition of product gas determines its quality as a fuel. High concentrations of combustible gasses such as carbon monoxide, hydrogen and methane increase the combustion energy of the product gas. India being agriculture based country that produces tonnes and tonnes of agriculture residue that can be utilized for to meet the rural energy demand which also contributes to environment protection. This study focuses in understanding the processes taking place in the biomass reactor also to investigate and model these reactions by considering a 100 kg/hr down draft biomass (wood) gasifier.

The aim of the present work is to predict the performance of the down draft biomass gasifier through computer simulation with computational fluid dynamics (CFD) software. The computation is then extended to study the variation in gas composition and calorific value of the producer gas while Increase the equivalence ration from 0.2 to 0.35 in steps of .05.

The results indicate that the calorific value of the producer gas increases as the equivalence ratio is increased from 0.20 to 0.30 and it attains maximum value at ER 0.3. Further it is noticeable that when the equivalence ratio increased beyond 0.3 there is a sharp decline in the calorific value of the gas.

CHAPTER 1

1.1 Introduction

Energy is one of the major inputs for the economic development of any country. In the case of the developing countries, the energy sector assumes a critical importance in view of the ever increasing energy needs requiring huge investments to meet them. Energy can be classified into several types based on the following criteria:

- Primary and Secondary energy
- Commercial and Non commercial energy
- Renewable and Non-Renewable energy

1.2 Primary and Secondary Energy

Primary energy sources are those that are either found or stored in nature. Common primary energy sources are coal, oil, natural gas, and biomass (such as wood). Other primary energy sources available include nuclear energy from radioactive substances, thermal energy stored in earth's interior, and potential energy due to earth's gravity. The major primary and secondary energy sources are shown in Figure 1.1 Primary energy sources are mostly converted in industrial utilities into secondary energy sources; for example coal, oil or gas converted into steam and electricity. Primary energy can also be used directly. Some energy sources have non energy uses, for example coal or natural gas can be used as a feedstock in fertiliser plants.

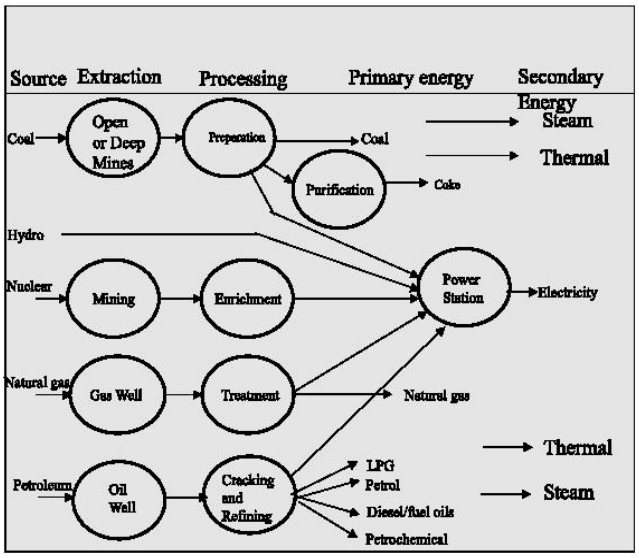

Figure 1.1 Major Primary and Secondary Sources

The energy sources that are available in the market for a definite price are known as commercial energy. By far the most important forms of commercial energy are electricity, coal and refined petroleum products. Commercial energy forms the basis of industrial, agricultural, transport and commercial development in the modern world. In the industrialized countries, commercialized fuels are predominant source not only for economic production, but also for many household tasks of general population. Examples: Electricity, lignite, coal, oil, natural gas etc.

Non-Commercial Energy

The energy sources that are not available in the commercial market for a price are classified as non-commercial energy. Non-commercial energy sources include fuels such as firewood, cattle dung and agricultural wastes, which are traditionally gathered, and not bought at a price used especially in rural households. These are also called traditional fuels. Non-commercial energy is often ignored in energy accounting.

Example: Firewood, agro waste in rural areas; solar energy for water heating, electricity generation, for drying grain, fish and fruits; animal power for transport, threshing, lifting water for irrigation, crushing sugarcane; wind energy for lifting water and electricity generation.

1.4 Renewable and Non-Renewable Energy

Renewable energy is energy obtained from sources that are essentially inexhaustible. Examples of renewable resources include wind power, solar power, geothermal energy, tidal power and hydroelectric power (See Figure 1.2). The most important feature of renewable energy is that it can be harnessed without the release of harmful pollutants.Non-renewable energy is the conventional fossil fuels such as coal, oil and gas, which are likely to deplete with time.

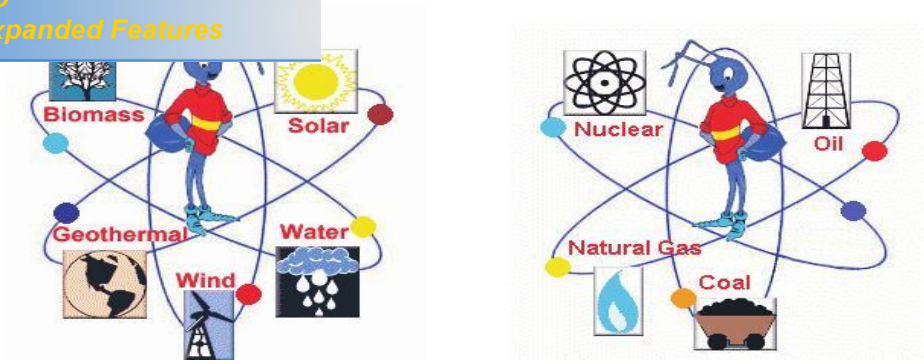

Renewable **Non Renewable**

Figure 1.2 Renewable and non renewable sources of energy

1.5 Global Primary Energy Consumption

The global primary energy consumption at the end of 2003 was equivalent to 9741 million tonnes of oil equivalent (Mtoe). The Figure 1.3 shows in what proportions the sources mentioned above contributed to this global figure.

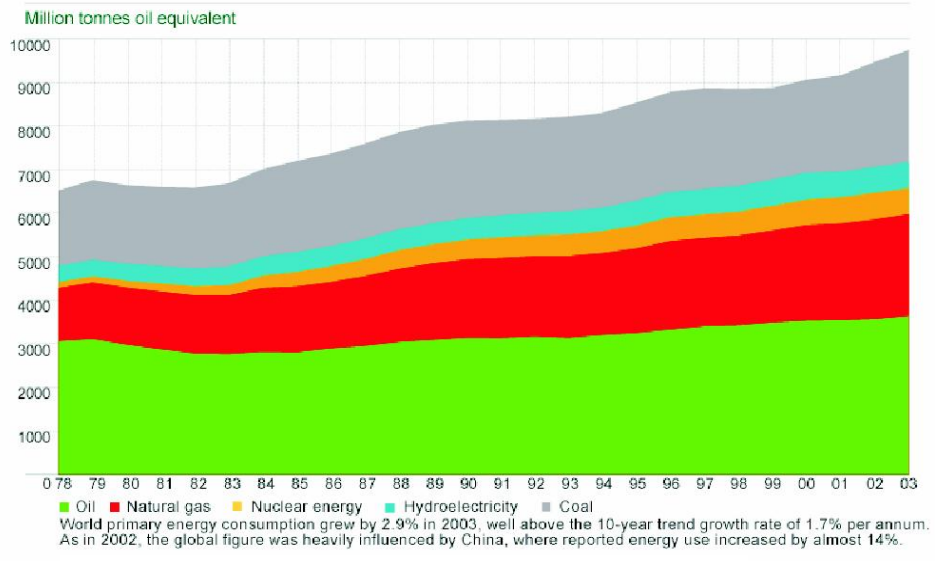

Figure 1.3 Global Primary Energy Consumption

umption for few of the developed and developing countries are shown in Table 1.1. It may be seen that India's absolute primary energy consumption is only 1/29th of the world, 1/7th of USA, 1/1.6th time of Japan but 1.1, 1.3, 1.5 times that of Canada, France and U.K respectively.

TABLE 1.1 PRIMARY ENERGY CONSUMPTION BY FUEL, 2003

In Million tonnes oil equivalent

Country	Oil	Natural gas	Coal	Nuclear	Hydro	Total energy electric
USA	914.3	566.8	573.9	181.9	60.9	2297.8
Canada	96.4	78.7	31.0	16.8	68.6	291.4
France	94.2	39.4	12.4	99.8	14.8	260.6
Russian Federation	124.7	365.2	111.3	34.0	35.6	670.8
United Kingdom	76.8	85.7	39.1	20.1	1.3	223.2
China	275.2	29.5	799.7	9.8	64.0	1178.3
India	113.3	27.1	185.3	4.1	15.6	345.3
Japan	248.7	68.9	112.2	52.2	22.8	504.8
Malaysia	23.9	25.6	3.2	-	1.7	54.4
Pakistan	17.0	19.0	2.7	0.4	5.6	44.8
Singapore	34.1	4.8	-	-	-	38.9
TOTAL WORLD	3636.6	2331.9	2578.4	598.8	595.4	9741.1

1.6 Energy Distribution Between Developed and Developing Countries

Although 80 percent of the world's population lies in the developing countries (a four fold population increase in the past 25 years), their energy consumption amounts to only 40 percent of the world total energy consumption. The high standards of living in the developed countries are attributable to high energy consumption levels. Also, the rapid population growth in the developing countries has kept the per capita energy consumption low compared with that of highly industrialized developed countries. The world average energy consumption per person is equivalent to 2.2 tonnes of coal. In industrialized countries, people use four to five times more than the world average, and nine times more than the average for the developing countries. An American uses 32 times more commercial energy

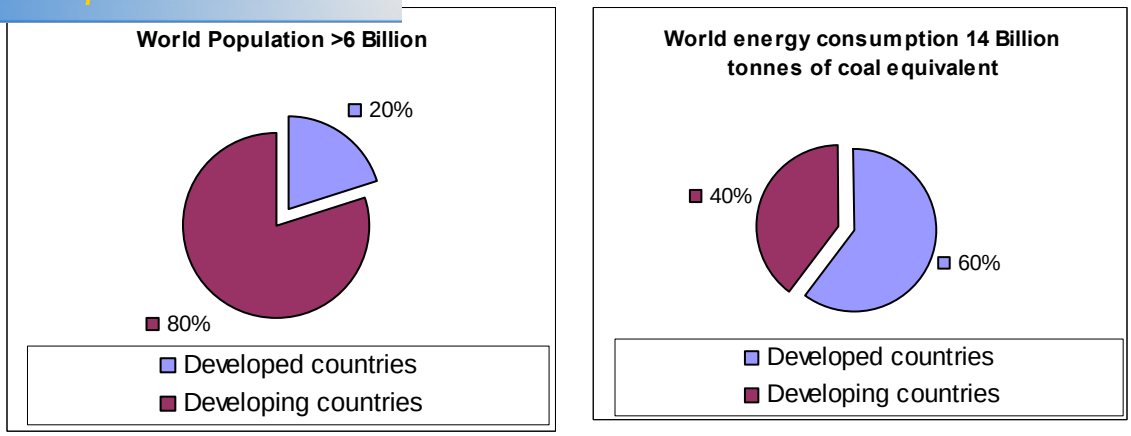

Figure 1.4: Energy Distribution between Developed and Developing Countries

d

The process of gasification to produce combustible from organic feeds was used in blast furnaces over 180 years ago. The possibility of using this gas for heating and power generation was soon realized and there emerged in Europe producer gas systems, which used charcoal and peat as feed material. At the turn of the century petroleum gained wider use as a fuel, but during both world wars and particularly World War II, shortage in petroleum supplies led to widespread re-introduction of gasification. By 1945 the gas was being used to power trucks, buses and agricultural and industrial machines. It is estimated that there were close to 9000,000 Vehicles running on producer gas all over the world.

After World War II the lack of strategic impetus and the availability of cheap fossil fuels led to general decline in the producer gas industry. However Sweden continued to work on producer gas technology and the work was accelerated after 1956 Suez Canal crisis. A decision was then made to include gasifiers in Swedish strategic emergency plans. Research into suitable designs of wood gasifiers, essentially for transport use, was carried out at the National Swedish Institute for Agricultural Machinery Testing and is still in progress. The contemporary interest in small scale gasifier R&D, for most part dates from 1973 oil crisis. The U.S. research in this area is reviewed by Goss11. The manufacturing also took off with increased interest shown in gasification technology. At present there are about 64 gasification equipment manufacturers all over the world.

Biomass gasification offers several potential advantages over alternative approaches. First, conversion of the solid feedstock to a gaseous fuel significantly increases the opportunities for using biomass as an energy source. Since the gasification product is a fuel or synthesis gas rather than simply a stream of hot combustion products, the fuel can be used for different purposes. When sufficiently cleaned, the product gas can be used for applications such as:

- Powering higher-efficiency (~40%) conversion devices such as gas turbines

oil- or natural gas-fired equipment to operate on

- Providing fuel for fuel cells or other distributed generation technologies
- Synthesizing liquid fuels, or chemicals

Gasification also offers potential environmental advantages when compared to combustion systems. The fuel gas produced by gasifiers is lower in both volume and temperature than the fully combusted product from a combustor. These characteristics provide an opportunity to clean and condition the fuel gas prior to use. Combustion of the resulting gaseous fuel can be more accurately controlled than combustion of the solid biomass. As a result, the overall emissions from gasification based power systems, particularly those of NOx, can be reduced. The ability to produce clean energy potentially allows gasification to be used in other situations where combustion is unsuitable including:

- Facilities where stringent emission standards are enforced
- Locations where public perception of combustors is negative

These combined advantages of flexibility and environmental compatibility make gasification a significant option for new, high-efficiency electricity generation applications and for the synthesis of liquid fuels from biomass. Biomass gasification has been a subject of interest for many decades. Historically, emphasis has been placed on small-scale gasifiers, and numerous designs have been built and tested.

The products from these gasifiers have been used in a variety of applications ranging from fuel for emergency vehicles during World War II to fuel for stationary heat and power generation today (National Research Council, 1983; Reed and Das, 1998; Klass, 1998; Quaak, et al, 1999; IEA Bioenergy, 1997; Barker, 1998; Costello and Chum, 1998; Stevens, 1999; BTG,2000). Over the past two decades, there has been increasing interest in the use of larger-scale gasifiers to provide fuels for advanced power generation concepts such as gas turbines, or for use where strict environmental emission regulations exist. In these cases, the raw product gas must be cleaned and conditioned prior to use. The characteristics of the raw

endent on the type of gasification process used
er. The basics of gasification

2.2 Basics of Biomass Gasification

At temperatures of approximately 600-1000 °C, solid biomass undergoes thermal decomposition to form gas-phase products that typically include carbon monoxide, hydrogen, methane, carbon dioxide, and water. In most cases, solid char plus tars that 4 would be liquids under ambient conditions are also formed. The product distribution and gas composition depends on many factors including the gasification temperature and the reactor type. The kinetics and mechanisms of biomass gasification have been studied extensively, and more extensive reviews of gasification can be found elsewhere (Karlschmitt and Bridgwater, 1997; Klass, 1998; Quaak, et al, 1998). As a result of many years of effort, numerous gasifiers have been designed and tested, mostly at small scale with capacities ranging from a few kilograms to a few tons of biomass feedstock per day. The selection of a particular design has a major influence on the primary characteristics of the product gas including its energy content, the concentrations of tars and particulates in the gas, and the relative amounts of various gaseous products such as hydrogen, carbon monoxide, and carbon dioxide.

2.3 Gasification Approaches

While the characteristics of the product gases from different concepts varies significantly, gasification approaches can be grouped into two general types based on the energy content of the product. The energy content of the gas depends on the approach used to supply heat to drive the gasification reactions. Most designs use oxygen, either in air or in its separated form, as an oxidizing agent to generate heat by partially combusting the biomass feedstock. When heat is supplied by partial oxidation with air (air-blown gasification), nitrogen in the air dilutes the product. The resulting gas is classified as a low-energy gas and has a heating value of approximately 2.5-8.0 MJ/Nm3. Low-energy gasifiers are best used in situations where the heat content of the gas is not a critical issue such as cofiring applications, district heating systems, and many electric generation systems. Medium-energy gases can be produced using pure oxygen instead of air as the oxidizing

the gasification. The use of separated oxygen uent, and a medium-energy gas (10-20 MJ/Nm3) can be produced. In the absence of oxygen, medium-energy gases can also be produced by pyrolytic gasification by using a reactor where heat for the gasification is provided from an external source (indirectly-fired gasification). In these gasifiers, heat is provided using methods such as heat exchangers and circulating the hot bed material. Medium-energy gasifiers are appropriate for situations where a higher energy-content gas is desired. The synthesis of liquid fuels requires the use of medium-energy gasifiers since these systems cannot effectively deal with the dilution of the product by nitrogen that occurs in air-blown systems.

2.4 Biomass energy conversion processes

Biomass is the solar energy stored in chemical form in plant and animal materials and is among the most precious and versatile resources on earth. It provides not only food but also energy, building materials, paper, fabrics, medicines and chemicals. Today, biomass fuels can be utilized for tasks ranging from heating to fuelling automobiles. In this respect, biomass is considered the renewable energy source with the highest potential to contribute to the energy needs of modern society for both the developed and developing economies world-wide because the prospects for production at competitive costs are vast. It is therefore important that the setbacks in the technologies for conversion of biomass into energy are improved upon. In considering the methods for extracting the energy, it is possible to order them by the processes that are discussed in the following:

2.4.1 Biological processing

This includes processes such as anaerobic digestion and fermentation which, lead to a useful gaseous or liquid fuel. Anaerobic digestion, like pyrolysis, occurs in the absence of air; but in this case the decomposition is caused by bacterial action rather than high temperatures. It is a process which takes place in almost any biological material that is decomposing and is favored by warm, wet and of course, airless conditions. In this case the resulting gas is a mixture consisting mainly of methane and carbon dioxide usually referred to as biogas.

ocessing to upgrade the bio-fuel

include pyrolysis, gasification and liquefaction. In Thermo-chemical processing, the equivalence ratio ū is an important parameter and is given by

$$\phi = \frac{\frac{m_{fuel}}{m_{oxygen}}}{\left(\frac{m_{fuel}}{m_{oxygen}}\right)_{Stoichiomatric}}$$

Where m_{fuel} is the mass of fuel and m_{oxygen} is the mass of oxygen.
The stoichiometric oxygen to fuel ratio is the theoretical amount of oxygen needed to completely combust the fuel. Based on the equivalence ratio, different types of thermal processes of biomass fuels are characterized as follows.

I) Pyrolysis: 0Ò ū Ò0.2

II) Combustion: ū Ó0.4

III) Gasification: 0.2Ò ū Ò0.40

2.4.3 Chemistry

The substance of a solid fuel is usually composed of the elements carbon, hydrogen and oxygen. In the gasifiers considered, the biomass is heated by combustion. Four different processes can be distinguished in gasification: drying, pyrolysis, oxidation and reduction.

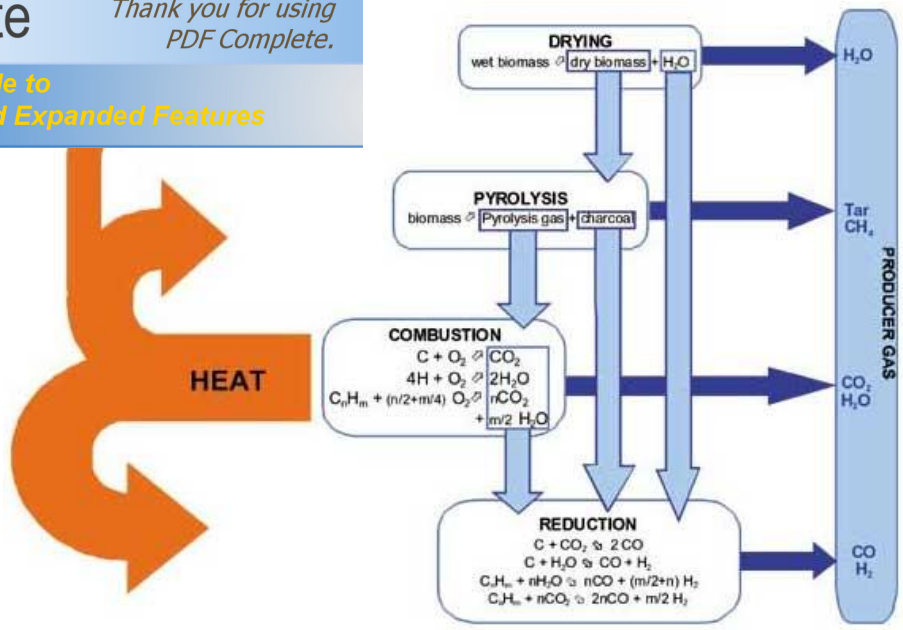

Fig 2.1 Chemistry of bio-mass gasification

The water gas shift reaction determines to a large extent the final gas composition. The equilibrium constant (Kw) can be written as. Kw =/ $[CO_2]$ x $[H_2]$ / [CO] x [$[H_2O]$ In practice, the equilibrium composition of the gas will only be reached in cases where the reaction rate and the time for reaction are sufficient. Below 700 ° the water-gas shift becomes so slow -without a catalyst- that the equilibrium is said to be 'frozen'. The gas composition then remains unchanged. Methane equilibrium will only be reached at very high temperatures (> 1200 °C).

2.5 Direct Gasification:

In direct gasification, Oxygen or Air is used as blast. Gasification can be accomplished by using the principal of partial oxidation. In this case exothermic gasification occurs by supplying sub-stoichiometric blast to the process. The equivalence ratio (ER) is the amount of oxidant supplied relative to the stoichiometric requirement. Optimum gasification efficiency occurs near an equivalence ratio of 0.26 in purely direct biomass gasification. In practical reality, incomplete conversion will occur due to kinetic limitations of volatile matter conversion and heat and mass transfer limitations of fixed carbon conversion. These affects relate to reactor design constraints and system configuration effects. The amount of tar in the generated gas often depends on reactor design. Minimizing tar with creative equipment design is a principal goal for gasification engineers.

:

omplished using steam as an oxidant. However, steam reforming of biomass is endothermic and often heat transfer limited. Endothermic gasification generates more methane than direct gasification per volume of gas, so the energy density may be higher.

The thermal input required for steam reforming of biomass means that some clever method of high rate heat transfer must be devised. Steam gasification is thermodynamically more efficient than direct gasification, but practical heat transfer limitations and thermodynamic availability requirements for high temperature heat exchange often makes reality a bit different.

2.7 Applications of Gasification:

- **Producer gas**

  It can be obtained from gasification and employed in thermal application or for mechanical / electrical power generation. Like any other gaseous fuel, producer gas affords much better control over power levels when compared to solid fuel. This also paves the way for more efficient and cleaner operation.

- **Thermal Applications**

  For thermal applications, gasifiers are a good option as they can be retrofitted with existing devices such as ovens, furnaces, boilers, etc. Thermal energy of the order of 4.5 to 5.0 MJ is released by burning 1 cubic meter of producer gas in the burner. Flame temperatures in the range of 1200° C can be obtained by optimal air preheating and pre-mixing of air with gas. A few of the devices which could be retrofitted with gasifiers are furnaces for melting non-ferrous metals and for heat treatment, tea dryers, ceramic kilns, boilers for process steam and thermal fluid heaters.

- **Power Generation**

  A diesel engine can be operated on dual fuel mode using producer gas. Diesel substitution of over 80% at high loads and 70 - 80% under normal load variations can be achieved. The mechanical energy thus

d either for driving water pumps for irrigation or for alternator for electrical power generation. Alternatively, a gas engine can be operated with producer gas on 100% gas mode with suitably modified air / fuel mixing and control system. This application places constraints on the tar content in the producer as high levels of tar content can damage and reduce the efficiency of the engine.

Theoretically, almost all kinds of biomass with moisture content of 5-30% can be gasified. However, not every biomass fuel can lead to the successful gasification. Most of the development work is carried out with common fuels such as coal, charcoal and wood. It was recognized that fuel properties such as surface, size, shape as well as moisture content, volatile matter and carbon content influence gasification.

2.8 TYPES OF REACTORS

Based on the design of gasifiers and type of fuels used, there exists different kinds of gasifiers. Portable gasifiers are mostly used for running vehicles. Stationary gasifiers combined with engines are widely used in rural areas of developing countries for many purposes including generation of electricity and running irrigation pumps. Technologies such biomass gasification that allows utilization of biomass fuel is of great importance. Hence for various fuels and output gas applications, different types of gasifiers are used. Some of the commonly used gasifiers are:

2.8.1 Updraft or Counter-current gasifier

It is one of the oldest and most simplified types of gasifier. In an updraft gasifier, the flow of the biomass particles and the gasification agent (i.e. air/oxygen/steam) is in opposite directions. The air intake is at the bottom and the gas leaves at the top. The combustion reactions occur at the grate that is near the bottom of the gasifier, which are followed by reduction reactions somewhat higher up in the gasifier. As shown in Figure 3.1; in the upper part of the gasifier, heating and pyrolysis of the feedstock occur as a result of heat

tion and radiation from the lower zones. The tars during this process are carried in the gas stream. Ashes are removed from the bottom of the gasifier.

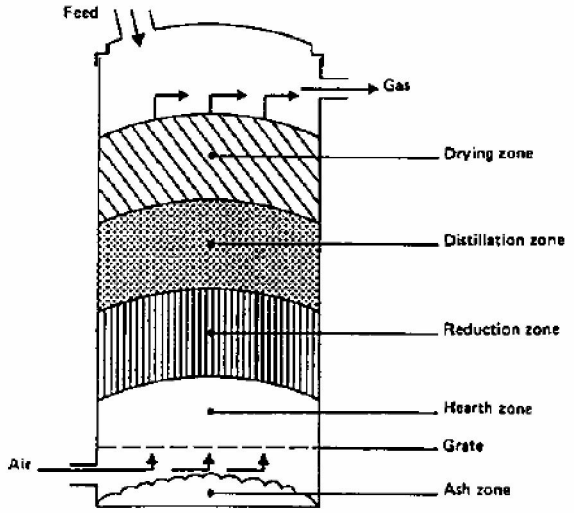

Figure 2.2: Updraft Gasifier

ges of this type of gasifier are its simplicity, high nternal heat exchange leading to low gas exit temperatures and high equipment efficiency. The drawback of an updraft gasifier is the high amount of tar content that is produced in the gasifier, which makes the producer gas unsuitable for engine applications.

2.8.2 Downdraft or Co-current gasifier

In a downdraft gasifier, the biomass material enters the gasifier through a hopper. In this type of gasifier, there is a co-current flow that gives discrete zones of pyrolysis and char gasification. On their way down the acid and tarry pyrolysis products from the fuel pass through a glowing bed of charcoal and therefore are converted into permanent gas i.e. a mixture of hydrogen, carbon dioxide, carbon monoxide and methane. Depending on the temperature of the hot zone and the residence time of the tar vapors, a near complete breakdown of the tars is achieved.

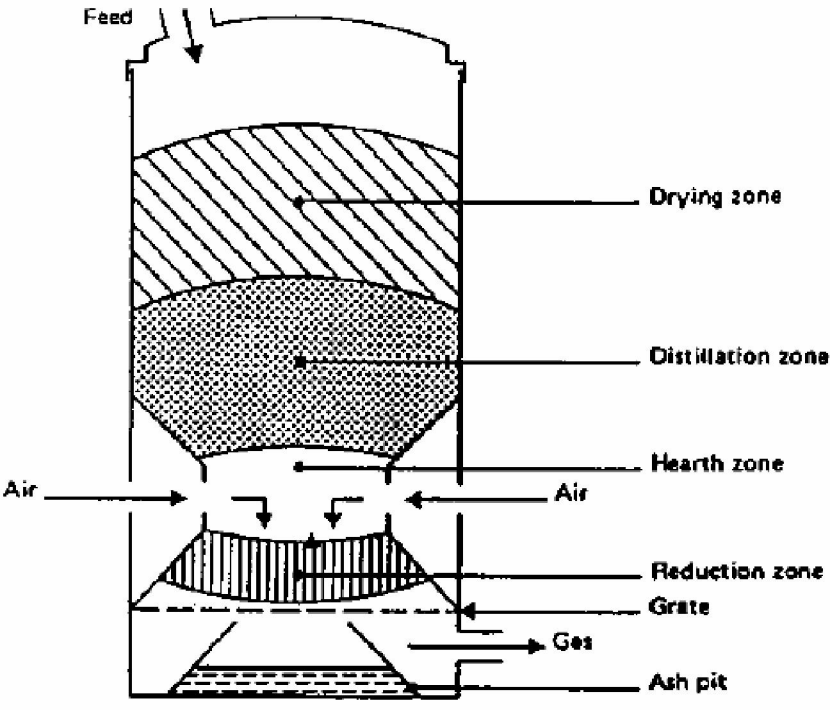

Figure 2.3: Downdraft Gasifier

e of downdraft gasifiers lies in the possibility of uitable for engine applications. However, practically it is highly improbable to achieve a tar-free gas. Also since the levels of organic compounds in condensate are lower for downdraft gasifier and hence it poses less threat to the environment. The major drawback of downdraft equipment lies in its inability to operate on a number of unprocessed fuels. In particular, fluffy and low-density materials give rise to flow problems and excessive pressure drop, and the solid fuel must be pelletized or briquetted before use. Minor drawbacks of the this type of system, as compared to updraft system, are somewhat lower efficiency resulting from the lack of internal heat exchange as well as the lower heating value of the gas.

2.8.3 Cross-draft gasifier

Cross-draft gasifiers are an adaptation for the use of charcoal. Charcoal gasification results in very high temperatures (1500 °C and higher) in the oxidation zone which places constraints on the material used for the structure of the gasifier. In cross draft gasifiers the fuel (charcoal) itself provides insulation against these high temperatures. Advantages of the system lie in the very small scale at which it can be operated. Installations below 10 kW (shaft power) can under certain conditions be economically feasible. The reason is the very simple gas-cleaning train (only a cyclone and a hot filter) which can be employed when using this type of gasifier in conjunction with small engines. A disadvantage of cross-draught gasifiers is their minimal tar-converting capabilities and the consequent need for high quality (low volatile content) charcoal.

2.8.4 Fluidized bed gasifier

The operation, of both up and downdraft gasifiers, is influenced by the morphological, physical and chemical properties of the fuel. Problems commonly encountered are: lack of bunkerflow, slagging and extreme pressure drop over the gasifier. As shown in Figure 3.3, air is blown through a bed of solid particles at a sufficient velocity to keep these in a state of suspension. The bed is originally externally heated and the feedstock is introduced as soon as a sufficiently high temperature is reached. The fuel particles are introduced at the bottom of the reactor, very quickly mixed with

almost instantaneously heated up to the bed of this treatment the fuel is pyrolyzed very fast, resulting in a component mix with a relatively large amount of gaseous materials. Further gasification and tar-conversion reactions occur in the gas phase. Most systems are equipped with an internal cyclone in order to minimize char blow-out as much as possible. Ash particles are also carried over the top of the reactor and have to be removed from the gas stream if the gas is used in engine applications.

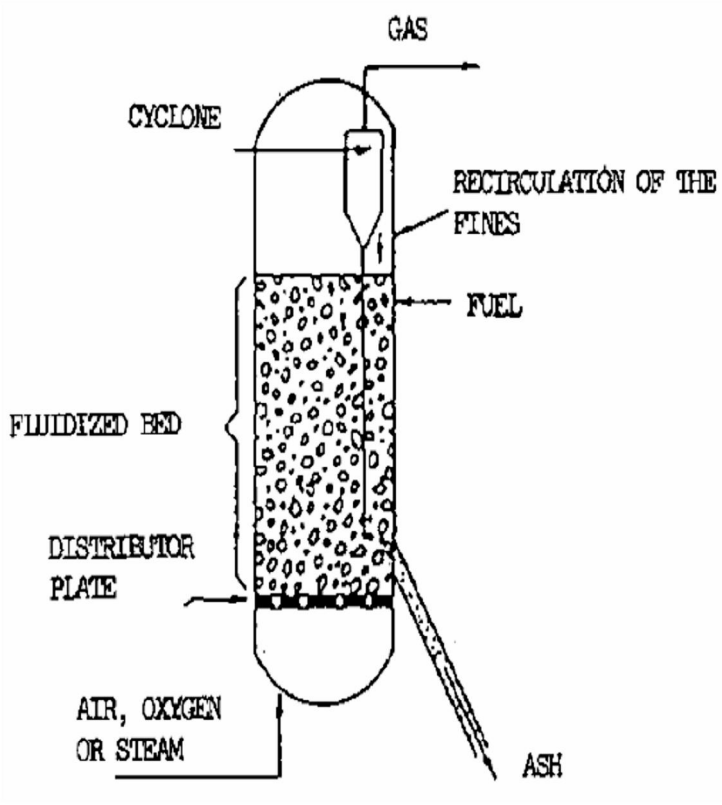

Figure 2.4: Fluidized Bed Gasifier

The major advantages of fluidized bed gasifiers come from their feedstock flexibility resulting from easy control of temperature, which can be kept below the melting or fusion point of the ash (rice husks), and their ability to deal with fluffy and fine grained materials (sawdust etc.) without the need of pre-processing. Problems with feeding, instability of the bed and fly-ash

nels can occur with some biomass fuels. Other bed gasifier lie in the rather high tar content of the product gas (up to 500 mg/m³ gas), the incomplete carbon burn-out, and poor response to load changes.

2.8.5 Rotary Kiln

In this type of gasifier, the charge is slowly tumbling which results in limited contact between the charge and the gas phase. Hence, Rotary Kiln gasifier has incomplete gasification unless conditions are favorable for long residence times of the charge in the gasifier.

2.8.6 Spouted bed

Spouted bed gasifier is a variant of the fluidized bed gasifier. There are multiple spouts present in the gasifier through which coarse material can be introduced in the bed. This kind of gasifier is capable of handling mixed biomass materials of different densities and sizes.

2.8.7 Entrained flow gasifiers

They are commonly used for coal because they can be slurry fed in direct gasification mode, which makes solid fuel feeding at high-pressures delightfully inexpensive. There are several commercial designs available for coal but these will not work with more than 10 to 15% biomass in a coal blend. This principal slurry feeding benefit can not be afforded to biomass because of its high porosity (lower energy density) and moisture holding capacity in a slurry phase. An entrained flow gasifier could be conceived that is pneumatically fed, for example for use with sawdust or other finely divided biomass. However, the pneumatically fed EFG does not compare to the high pressure feeding benefits achieved by slurry feeding. There is one company that has hinted at using an entrained flow concept for biomass, namely Emery Energy, but details are not publicly available. ETFGs can operate in slagging and non-slagging modes, referring to either molten ash or dry ash production. Slagging gasification is not practical for biomass due to its lower go/no-go ash fusion limits.

2.9 CHEMICAL KINETICS OF GASIFICATION

During the process of biomass gasification, various chemical and physical processes occur simultaneously. It is necessary to model the kinetics of these systems to conduct an accurate simulation of a biomass gasifier. The following processes are the major phenomena which occur:

2.9.1 Pre Heating

This involves pre-heating of the fuel and air for better gasification.

2.9.2 Drying

Drying is first major process occurring inside the gasifier. It takes place at nearly 50-150 C where all the moisture in the wood is converted into steam. The steam helps in reduction further down the system. The rate of drying is affected by numerous factors such as Temperature, velocity of the feed, moisture content, external surface area and diffusivity.

2.9.3 Devolatilization

In the devolatilization (pyrolysis) zone, the volatile components which are present in the wood, including various aromatic and tarry compounds, get vaporized and the remaining wood gets converted into char. Typically, pyrolysis occurs at 200-800 C and produces char, carbon monoxide, carbon dioxide, water vapor, methane, other higher hydrocarbons, pyroligneous acids and tars. Pyrolysis is affected by various factors such as pyrolysis temperature, rate of heating, physical & chemical characteristics of feed and presence of catalytic compounds.

2.9.4 Gasification

In the gasification process, primarily the char and other solid/liquid organic compounds gets reduced and oxidized to form various gases which make up the output gas. This is one of the key processes in the process of Biomass gasification and optimization of this process can help in increasing the calorific

...e same time reducing the amount of tar content in

2.9.5 Miscellaneous processes

In addition to the above processes, various other processes occur in the gasifier like consecutive gas phase reaction involving water shift reaction, steam reforming reaction and also other various other ash-catalyzed reactions.

2.10 Chemical Reactions

In a biomass gasifier, various chemical reactions take place inside the system. These reactions can be broadly divided into 2 categories i.e. homogenous reaction and non-homogenous (heterogeneous) reactions:

- **Heterogeneous reactions:**
  These reactions involve reactions occurring in multiple phases. In a gasifier, many solid-gas reactions occur in the gasification zone that comes under this category. Some of these reactions include:

  C + CO2 = 2CO2 ---------- (1)

  C + H2O = CO + H2 ---------- (2)

  C + H2 = CO + H2O ---------- (3)

  C + 2H2 = CH4 ---------- (4)

  C + 3H2 = CH4 + H2O ---------- (5)

- **Homogenous reactions:**
  The homogenous reactions occur in a single phase and mainly constitute of gas phase reactions including:

  $H_2 + O_2$ Ÿ H_2O---------- (6)

  $CO_2 + H_2$ Ÿ $CO + H_2O$---------- (7)

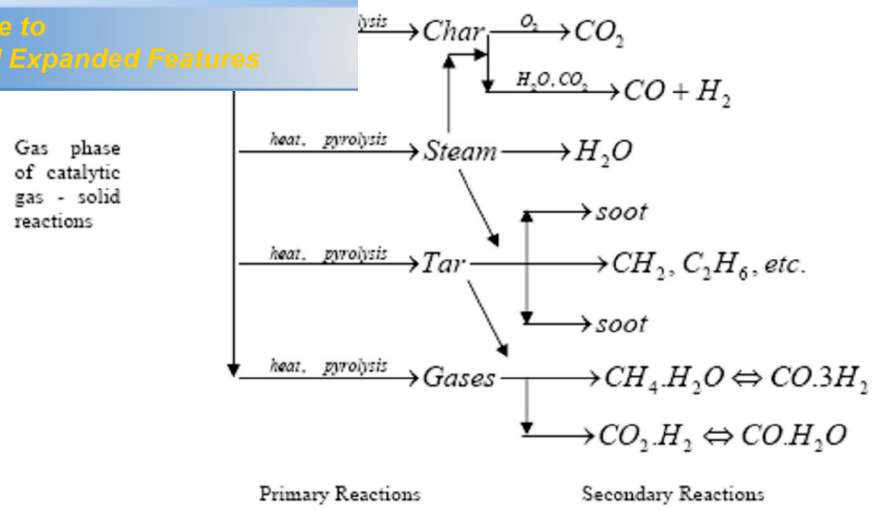

Figure 2.5 shows the how the various physical and chemical reaction occur in a gasifier in a series and parallel system.

A typical composition of the gas obtained from wood gasification on volumetric basis is as follows:

Carbon monoxide	: 18% - 22%
Hydrogen	: 13% - 19%
Methane	: 1% - 5%
Heavier hydrocarbons	: 0.2% - 0.4%
Carbon dioxide	: 9% - 12%
Nitrogen	: 45% - 55% and
Water vapour	: 4%

The calorific value of the producer gas is about 1 000 ï 1 200 kcal /Nm3. Approximately 2.5 Nm3 of producer gas is obtained from the gasification of one kilogram of biomass. The sequence of these reactions in a downdraft gasifier is shown in Figure 3.5. The drying and pyrolysis reactions occur at the top of the gasifier. In the central zones of the gasifier, which attain a peak temperature in the gasifier, air (which might be pre-heated or not) enters the system through tuyeres (i.e. nozzles). This is the oxidation zone in the gasifier and this is followed by primary and secondary reduction zones.

With the help of the above reaction scheme, and with knowledge of the equilibrium constants, it is possible to predict the equilibrium composition of the gaseous products. The equilibrium composition of a given solid fuel

y per unit weight of the biomass. A dimensionless R (equivalence ratio), is applied to characterize the air supply conditions, and is usually defined as follows:

$$ER = \frac{\text{(Weight of oxygen/ Weight of dry fuel)}}{\text{(Weight of oxygen/ Weight of dry fuel)}_{\text{stiochiometric}}}$$

The denominator in the above equation is the oxygen required for complete combustion of the fuel and it varies from fuel to fuel. It is generally observed that for effective gasification, the ER should be in the range of 0.2 - 0.4. Below an ER value of 0.2, pyrolysis pre-dominates the process and above an ER value of 0.4, combustion predominates.

Based on the discussion in this chapter, comprehensive gasifier models will be developed and tested in the following chapters. The main emphasis of the simulation would be on analyzing the effect of various operational parameters on the system characteristics and the gas quality in a fixed bed reactor (prominent focus on downdraft gasification).

2.11 Factors affecting gasification

Studies have shown that there are several factors influencing the gasification of wood. These include the following:

2.11.1 Energy content of Fuel

Fuel with high energy content provides easier combustion to sustain the endothermic gasification reactions because they can burn at higher temperatures. Beech wood chips have an energy content of approximately 20 MJ/kg. This is typical for most biomass sources and has been proved to be easy to gasify.

2.11.2 Fuel Moisture content

Since moisture is in effect water, a non-burnable component in the biomass, it is important that the water content be kept to a minimum. All water in the feed stock must be vaporized in the drying phase before combustion otherwise there will be difficulty in sustaining combustion because the heat released will be used to evaporate moisture. Wood with low moisture content can therefore

an that with high moisture. Wood with high dried first before it can be used as fuel for the gasifier. The beech wood chips used in the experiments have been factory dried to a moisture content of 10% prior to packaging. This makes it suitable as a fuel for the gasifier .Updraft gasifiers are also capable of operating with fuels that have moisture contents of up to 50%.

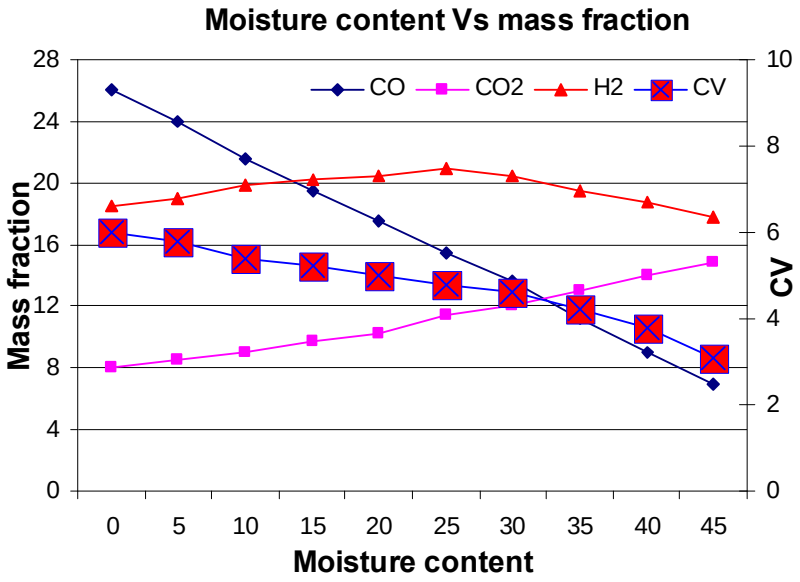

Fig 2.6 Fuel moisture content Vs calorific value

2.11.3 Size Distribution of the Fuel

Fuel should be of a form that will not lead to bridging within the reactor. Bridging occurs when unscreened fuels do not flow freely axially downwards in the gasifier. Therefore particle size is an important parameter in biomass gasification because it determines the bed porosity and thus the fluid-dynamic characteristics of the bed. On the other hand, fine grained fuels lead to substantial pressure drops in fixed bed reactors. The experimental wood chips are approximately 10 x 10 x 2 mm and regular in shape. This size is not fine grained when compared to the micron scale and thus no substantial pressure drops occur in the reactor.

Reactor

insulate the reactor so that heat losses are reduced. If heat losses are higher than the heat requirement of the endothermic reactions, the gasification reactions will not occur. The reactor in the laboratory has been insulated with 50 mm of alkaline earth silicate to keep heat losses minimal.

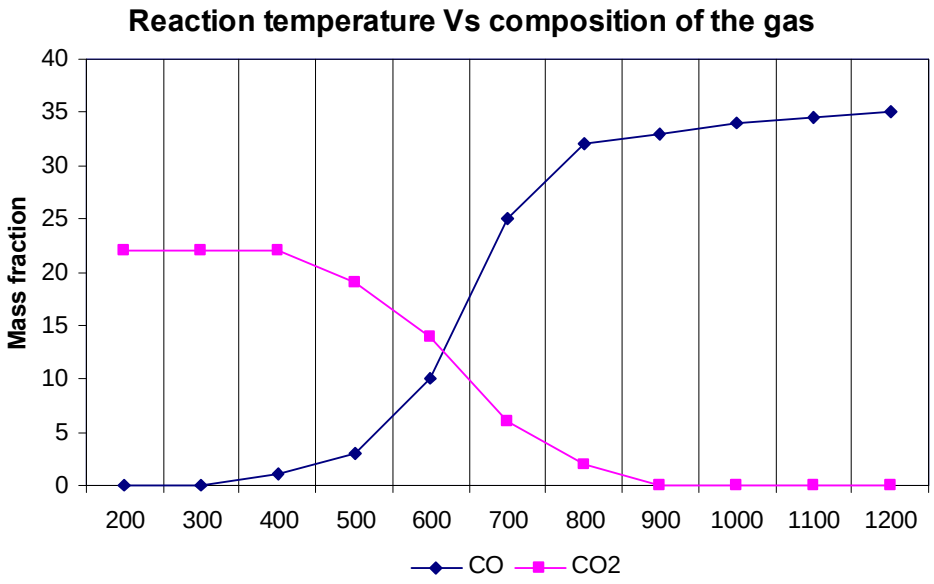

Fig 2.7 Temperature Vs composition of the Gas

r used in the simulation is shown in Fig 3.1. The gasifier is divided into two regions: a combustion region (combustor) in the second or the upper stage and a reduction region (reductor) in the first or the lower stage. The gasifier has two levels of air injectors that are positioned symmetrically. The upper and the lower injectors are aimed directly at the center of the fire box.

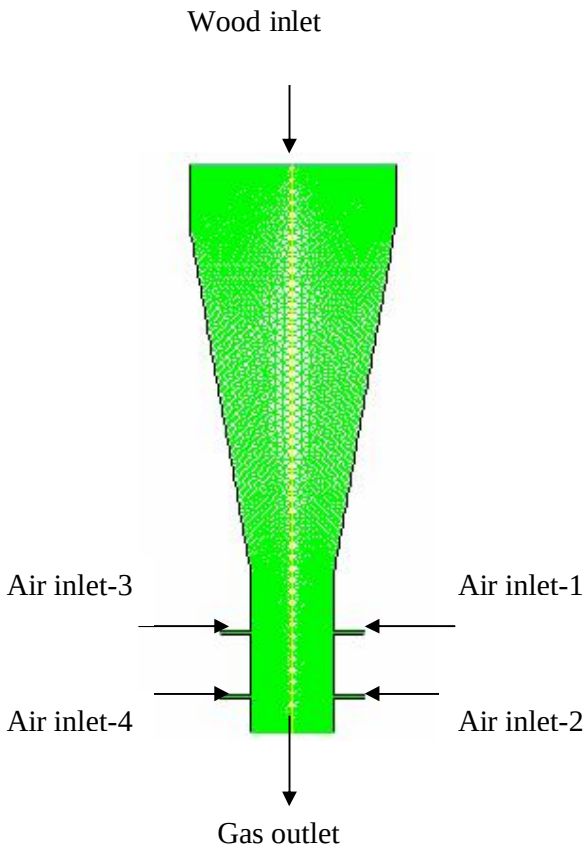

Fig: 3.1 Schematic of a down draft gasifier

3.1 Physical Characteristics of the Problem and Assumptions Made

The physical characteristics of the problem are as follow:

1. Two-dimensional
2. Bouyancy force considered
3. Varying fluid properties
4. Impermeable walls

The following are the general assumptions made in this study:

1. The flow is steady.
2. No-slip condition (zero velocity) is imposed on wall surfaces.
3. Chemical reaction is faster than the time scale of the turbulence eddies.

3.2 Governing Equations

The equations for conservation of mass, conservation of momentum, and energy equation are given as:

$$\nabla . \left(\rho \vec{v}\right) = S_m \longrightarrow \quad (3.1)$$

$$\nabla . \left(\rho \vec{v}\vec{v}\right) = -\nabla p + \nabla . \left(\bar{\bar{\tau}}\right) + \rho \vec{g} + \vec{F} \longrightarrow \quad (3.2)$$

$$\nabla . \left(v\left(\rho E + p\right)\right) = \nabla . \left(\lambda_{eff} \nabla T - \sum hjJj + \left(\vec{\tau}_{eff} . \vec{v}\right)\right) + S_h \longrightarrow \quad (3.3)$$

Where *is* λ_{eff} the effective conductivity (*l*+*lt*, where *lt* is the turbulence conductivity) and *Jj* is the diffusion of species *j*.

The stress tensor is given by

$$\bar{\bar{\tau}} = \mu \left[\left(\nabla \vec{v} + \nabla \vec{v}^{T} \right) - \frac{2}{3} \nabla . \vec{v} I \right] \longrightarrow \quad (3.4)$$

where *m* is the molecular dynamic viscosity, *I* is the unit tensor, and the second term on the right-hand side is the effect of volume dilatation. The first three terms on the right hand side of equation (3.3) represent heat transfer due to conduction, species diffusion, and viscous dissipation. *Sh* is a source

formation from the chemical reaction of the

efined as

$$E = h - \frac{P}{\rho} + \frac{v^2}{2} \longrightarrow (3.5)$$

where *h* is the sensible enthalpy and for incompressible flow and is given as

$$h = \sum_j Y_j h_j + \frac{p}{\rho} \longrightarrow (3.6)$$

Y_j is the mass fraction of species *j* and

$$h = \int_{Tref}^{T} C_{p_j} \, dT \longrightarrow (3.7)$$

where T_{ref} is 298.15 K.

3.3 Turbulence Model

The velocity field in turbulent flows always fluctuates. As a result, the transported quantities such as momentum, energy, and species concentration fluctuate as well. The fluctuations can be small scale and high frequency, which is computationally expensive to be directly simulated. To overcome this, a modified set of equations that are computationally less expensive to solve can be obtained by replacing the instantaneous governing equations with their time-averaged, ensemble-averaged, or otherwise manipulated to remove the small time scales. However, the modifications of the instantaneous governing equations introduce new unknown variables. Many turbulence models have been developed to determine these new unknown variables in terms of known variables. General turbulence models widely available are:

a. Spalart-Allmaras

b. *k-e* models:

- Standard *k-e* model
- RNG *k-e* model
- Realizable *k-e* model
- *k-w* model
- Standard *k-w* model
- Shear-stress transport (SST) *k-w* model

The standard *k-e* turbulence model, which is the simplest two-equation turbulence model, is used in this simulation due to its suitability for a wide range of wall-bound and free shear flows. The standard *k-e* turbulence is based on the model transport equations for the turbulence kinetic energy, *k*, and its dissipation rate, *e*. The model transport equation for *k* is derived from the exact equation; however, the model transport equation for *e* is obtained using physical reasoning and bears little resemblance to its mathematically exact counterpart.

The standard *k-e* turbulence model is robust, economic for computation, and accurate for a wide range of turbulent flows. The turbulence kinetic energy, *k*, and its rate of dissipations, *e*, are calculated from the following equations

$$\frac{\partial}{\partial x_i}(\rho k u_i) = \frac{\partial}{\partial x_j}\left[\left(\mu + \frac{\mu}{\sigma_k}\right)\frac{\partial k}{\partial x_j}\right] + G_k + G_b - \rho\varepsilon - Y_M + S_k \longrightarrow \quad (3.8)$$

and

$$\frac{\partial}{\partial x_i}(\rho \varepsilon u_i) = \frac{\partial}{\partial x_j}\left[\left(\mu + \frac{\mu}{\sigma_\varepsilon}\right)\frac{\partial \varepsilon}{\partial x_j}\right] + C_{1\varepsilon}\frac{\varepsilon}{k}(G_k + C_{3\varepsilon}G_b) - C2\varepsilon\rho\frac{\varepsilon^2}{k} + S_\varepsilon \longrightarrow \quad (3.9)$$

In equations (3.8) and (3.9), G_k represents the generation of turbulence kinetic energy due to the mean velocity gradients and is defined as

$$G_k = -\overline{\rho u'_i \bar{u}'_j}\frac{\partial u_j}{\partial x_j} \longrightarrow \quad (3.10)$$

G_b represents the generation of turbulence kinetic energy due to buoyancy and is calculated as

$$G_b = \beta g_i \frac{\mu_t}{\mathrm{Pr}_t}\frac{\partial T}{\partial x_i} \longrightarrow \quad (3.11)$$

Pr_t is the turbulent Prandtl number and g_i is the component of the gravitational vector in the *i*-th direction. For standard *k-e* model the value for Pr_t is set 0.85 in this study. The coefficient of thermal expansion, *b*, is given as

Y_M $\beta = -\frac{}{\rho}\left(\frac{}{\partial T}\right)_p$ represents the (3.12) ion of the fluctuating dilatation in compressible turbulence to the overall dissipation rate, and is defined as

$$Y_M = 2\rho\varepsilon M_t^2 \longrightarrow (3.13)$$

where M_t is the turbulent Mach number which is defined as

$$M = \sqrt{\frac{k}{a^2}} \longrightarrow (3.14)$$

where a $\left(\sqrt{\gamma RT}\right)$ is the speed of sound.

The turbulent viscosity, m_k, is calculated from equation

$$\mu_k = \rho C_\mu \frac{k^2}{\varepsilon} \longrightarrow (3.15)$$

The values of constants C_{1e}, C_{2e}, C_m, s_k, and s_e used are $C_{1e} = 1.44$, $C_{2e} = 1.92$, $C_m = 0.09$, $s_k = 1.0$, $s_e = 1.3$.

The turbulence models are valid for the turbulent core flows, i.e. the flow in the regions somewhat far from walls. The flow very near the walls is affected by the presence of the walls. Viscous damping reduces the tangential velocity fluctuations and the kinematic blocking reduces the normal fluctuations. The solution in the near-wall region can be very important because the solution variables have large gradients in this region. However, the solution in the boundary layer is not important in this study. Therefore, the viscous sublayer, where the solution variables change most rapidly, does not need to be solved. Instead, wall functions, which are a collection of semi-empirical formulas and functions, are employed to connect the viscosity-affected region between the wall and the fully-turbulent region. The wall functions consist of:

- laws-of-the-wall for mean velocity and temperature (or other scalars)
- formulas for near-wall turbulent quantities

function: (a) standard wall function and (b) n. The former is employed in this study. The wall function for the momentum is expressed as

$$U^+ = \frac{1}{k} In\left(Ey^+\right) \longrightarrow \quad (3.16)$$

$$U^+ = \frac{U_p C_\mu^{\frac{1}{4}} k_p^{\frac{1}{2}}}{\frac{\tau}{\rho}} \longrightarrow \quad (3.17)$$

$$y^+ \equiv \frac{\rho\, C_\mu^{\frac{1}{4}} k_p^{\frac{1}{2}} y_p}{\mu} \longrightarrow \quad (3.18)$$

and

k = von Karman constant (= 0.42)

E = empirical constant (= 9.793)

U_P = mean velocity of fluid at point P

k_P = turbulence kinetic energy at point P

y_P = distance from point P to the wall

m = dynamic viscosity of the fluid.

The wall function for the temperature is given as

$$T^+ \equiv \frac{(T_w - T_P)\rho c_P C_\mu^{\frac{1}{4}} k_P^{\frac{1}{2}}}{q} = \left\{ \Pr y^+, y^+ \left\langle y_T^+ \Pr\left[\frac{1}{k} In\left(Ey^+\right) + P\right], y^+ \right\rangle y_T \right\} \longrightarrow \quad (3.19)$$

$$P \equiv 9.24\left[\left(\frac{\Pr}{\Pr_T}\right)^{\frac{3}{4}} - 1\right]\left[1 + 0.28\, e^{\frac{-0.007\,\Pr}{\Pr_T}}\right] \longrightarrow \quad (3.20)$$

and

r = density of the fluid

c_p = specific heat of fluid

q = wall heat flux

T_P = temperature at cell adjacent to the wall

T_W = temperature at the wall

Pr = molecular Prandtl number

$\Pr_t$ = turbulent Prandtl number (0.85 at the wall)

t)

nstant)

E = 9.793 (wall function constant)

U_c = mean velocity magnitude at $y_+ = y_{+T}y_+$

T = non-dimensional thermal sublayer thickness.

The species transport is assumed to behave analogously to the heat transfer. The equation is expressed as

$$Y^+ \equiv \frac{\left(Y_{i,w} - Y_i\right)\rho c_P C_\mu^{\frac{1}{4}} k_P^{\frac{1}{2}}}{J_{i,w}} = \left\{ Scy^+, y^+ < y_c^+ \left\langle Sc_t\left[\frac{1}{k} In\left(Ey^+\right) + P_c\right], y^+ \right\rangle > y_T \right\} \longrightarrow \quad (3.21)$$

where Y_i is the local mass fraction of species i, Sc and Sc_t are the Schmidt numbers, and $J_{i,w}$ is the diffusion flux of species i at the wall. The turbulent Schmidt number, Sc, is given as $rD\ m$, where m is the viscosity and D is the diffusivity. The P_c and $y_{+\,c}$ are calculated in a similar way as P and $y^+{}_T$, with the difference being that the Prandtl numbers are replaced by the corresponding Schmidt numbers. In the k-e model, the k equation is solved in the whole domain, including the wall adjacent cells. The boundary condition for k imposed at the wall is

$$\frac{\partial k}{\partial \eta} = 0 \longrightarrow \quad (3.22)$$

where n is the local coordinate normal to the wall. The production of kinetic energy, G_k, and its dissipation rate, e, at the wall-adjacent cells, which are the source terms in k equation, are computed on the basis of equilibrium hypothesis with the assumption that the production of k and its dissipation rate assumed to be equal in the wall-adjacent control volume. The production of k and e is computed as$_{p\ P\ w}$

$$G_k \approx \tau_w \frac{\partial U}{\partial y} = \tau_w \frac{\tau_w}{k\rho C_\mu^{\frac{1}{4}}\ k_p^{\frac{1}{4}} y_p} \longrightarrow \quad (3.23)$$

$$\varepsilon_p = \tau_w \frac{C_\mu^{\frac{3}{2}}\ k_p^{\frac{3}{2}}}{k y_p} \longrightarrow \quad (3.24)$$

used to calculate the flux of the radiation at the inside walls of the gasifier. The P-1 radiation model is the simplest case of the more general PN radiation model that is based on the expansion of the radiation intensity *I*. The P-1 model requires only a little CPU demand and can easily be applied to various complicated geometries. It is suitable for applications where the optical thickness *aL* is large where *a* is the absorption coefficient and *L* is the length scale of the domain. The heat sources or sinks due to radiation is calculated using the equation

$$-\nabla q_r = aG - 4aG\sigma T^4 \longrightarrow \quad (3.25)$$

$$q_r = -\frac{1}{3(1+\sigma_s)-C\sigma_s}\nabla G \longrightarrow \quad (3.26)$$

and q_r is the radiation heat flux, a is the absorption coefficient, s_s is the scattering coefficient, G is the incident radiation, C is the linear-anisotropic phase function coefficient, and s is the Stefan-Boltzmann constant.
The flux of the radiation, $q_{r,w}$, at walls caused by incident radiation G_w is given as

$$q_{r,w} = -\frac{4\pi\varepsilon_w \frac{\sigma T_w^4}{\pi} - (1-\rho_w)G_w}{2(1+\rho_w)} \longrightarrow \quad (3.27)$$

$$\varepsilon_w = 1-\rho_w \longrightarrow \quad (3.28)$$

and r_w is the wall reflectivity.

3.5 Combustion Model

The global reaction mechanism is modeled to involve the following chemical species: C, O_2, N_2, CO, CO_2, H_2O and H_2 (see reactions R1.1 through R1.5 in Chapter 2). All of the species are assumed to mix in the molecular level. The chemical reactions inside the gasifier are modeled by calculating the transport and mixing of the chemical species by solving the conservation equations describing convection, diffusion, and reaction of each component species. The general form of the transport equation for each species is defined as

$$\left.\right) = -\nabla . \vec{J} + R_i \longrightarrow (3.29)$$

R_i is the net rate of production of species i by chemical reaction. $_i J_r$ is the diffusion fluxof species i, which arises due to concentration gradients. Mass diffusion for laminar flowsis given as

$$\vec{J} = -\left(\rho D_{i,m} + \frac{\mu_i}{Sc_i} \right) \nabla Y_i \longrightarrow (3.30)$$

For turbulent flows, mass diffusion flux is given as

$$\vec{J} = -\rho D_{i,m} \nabla Y_i \longrightarrow (3.31)$$

where Sc_t is the turbulent Schmidt number.

So, the transport equations for each chemical species are

$$\frac{\partial}{\partial t}(\rho Y_C) + \nabla\left(\rho \bar{v} Y_C\right) = -\nabla . \bar{J}_C + R_C \longrightarrow (3.32a)$$

$$\frac{\partial}{\partial t}(\rho Y_{O2}) + \nabla\left(\rho \bar{v} Y_{O2}\right) = -\nabla . \bar{J}_{O2} + R_{O2} \longrightarrow (3.32b)$$

$$\frac{\partial}{\partial t}(\rho Y_{N2}) + \nabla\left(\rho \bar{v} Y_{N2}\right) = -\nabla . \bar{J}_{N2} + R_{N2} \longrightarrow (3.32c)$$

$$\frac{\partial}{\partial t}(\rho Y_{CO}) + \nabla\left(\rho \bar{v} Y_{CO}\right) = -\nabla . \bar{J}_{CO} + R_{CO} \longrightarrow (3.32d)$$

$$\frac{\partial}{\partial t}(\rho Y_{CO2}) + \nabla\left(\rho \bar{v} Y_{CO2}\right) = -\nabla . \bar{J}_{CO2} + R_{CO2} \longrightarrow (3.32e)$$

$$\frac{\partial}{\partial t}(\rho Y_{H2O}) + \nabla\left(\rho \bar{v} Y_{H2O}\right) = -\nabla . \bar{J}_{H2O} + R_{H2O} \longrightarrow (3.32f)$$

$$\frac{\partial}{\partial t}(\rho Y_{H2}) + \nabla\left(\rho \bar{v} Y_{H2}\right) = -\nabla . \bar{J}_{H2} + R_{H2} \longrightarrow (3.32g)$$

t need to be solved are given below.

---------- (3.33)

C + H2O = CO + H2 ---------- (3.34)

C + H2 = CO + H2O ---------- (3.35)

C + 2H2 = CH4 ---------- (3.36)

C + 3H2 = CH4 + H2O ---------- (3.37)

There are three approaches to solving these reactions.

(a) Eddy-dissipation model: The assumption in this model is that the chemical reaction is faster than the time scale of the turbulence eddies. Thus, the reaction rate is determined by the turbulence mixing of the species. The reaction is assumed to occur instantaneously when the reactants meet.

(b) Equilibrium model: The rate of chemical reaction is governed by the rate of mixing of gaseous oxidant and reactant. The reactions are fast compare to the time scale of turbulence. The gaseous properties become functions of the turbulent mixing rate and can be calculated using equilibrium considerations [Fletcher, 1983].

(c) Reaction rate model: The rate of chemical reaction is computed using an expression that takes into account temperature and pressure and ignores the effects of the turbulent eddies. In this study, the eddy-dissipation model is used. The sources term R_i in equation (2.29) is calculated using the eddy-dissipation model based on the work of Magnussen and Hjertager [Magnusses et al., 1976]. The net rate of production or destruction of species *i* as the result of reaction *r*, $R_{i,r}$, is given by the smaller of the two expressions below.

$$R_{i,r} = v'_{i,r} M_{i,r} A \rho \frac{\varepsilon}{k} \min_R \left(\frac{Y_r}{v'_{R,r}, M_{w,j}} \right) \longrightarrow \quad (3.38)$$

$$R_{i,r} = v'_{i,r} M_{i,r} B \rho \frac{\varepsilon}{k} \left(\frac{\sum_p Y_P}{\sum_j^N v''_{j.r} M_{w,j}} \right) \longrightarrow \quad (3.39)$$

where,

Y_P is the mass fraction of any product species, *P*

Y_R is the mass fraction of a particular reactant, *R*

tant equal to 4.0

tant equal to 0.5

$v'_{i,r}$ is the stoichiometric coefficient of reactant *i* in reaction *r*

$v''_{j,r}$ is stoichiometric coefficient of product *j* in reaction *r*.

In equations (3.12) and (3.13), the chemical reaction rate is governed by large eddy mixing time scale, k/ε. The smaller of the two expressions (3.12) and (3.13) is used because it is the limiting value that determines the reaction rate. The procedure to solve the reactions is as follows.

1. The net local production or destruction of species *i* in each reaction is calculated by solving equations (3.12) and (3.13).
2. The smaller of these values is substituted into the corresponding species transport equation (3.10) to calculate the local species mass fraction, Y_i.
3. Y_i is then used in equation (3.11) to calculate the net enthalpy production of each reaction equation.
4. The net enthalpy production becomes the source term in energy equation (3.3) that affects the temperature distribution. In an endothermic process, the net enthalpy production is negative, which becomes a sink term in the energy equation.

s: Figure 3.2 shows the boundary conditions for e down draft biomass gasifier. Boundary conditions for all the cases simulated in this study are summarized in Table 3.1.

	Case 1	Case 2	Case 3	Case 4
Fuel Mass flow rate (kg/s)	0.013889	0.013889	0.013889	0.013889
Temperature (K)	300	300	300	300
Air				
Mass flow rate of (kg/s)	0.0185	0.0231	0.0277	0.0323
Tier 1(kg/s)	0.0092	0.0115	0.0138	0.0162
Tier 2 (kg/s)	0.0092	0.0115	0.0138	0.0162
Temperature (K)	600	600	600	600
Equivalence ratio (Ø)	0.2	0.25	0.30	0.35
Fuel Mass fraction at inlet	C: 0.53 H: 0.06 O: 0.41	C: 0.53 H: 0.06 O: 0.41	C: 0.53 H: 0.06 O: 0.41	C: 0.53 H: 0.06 O: 0.41

Table 3.1 Flow and Boundary conditions

Boundary conditions: Case-1

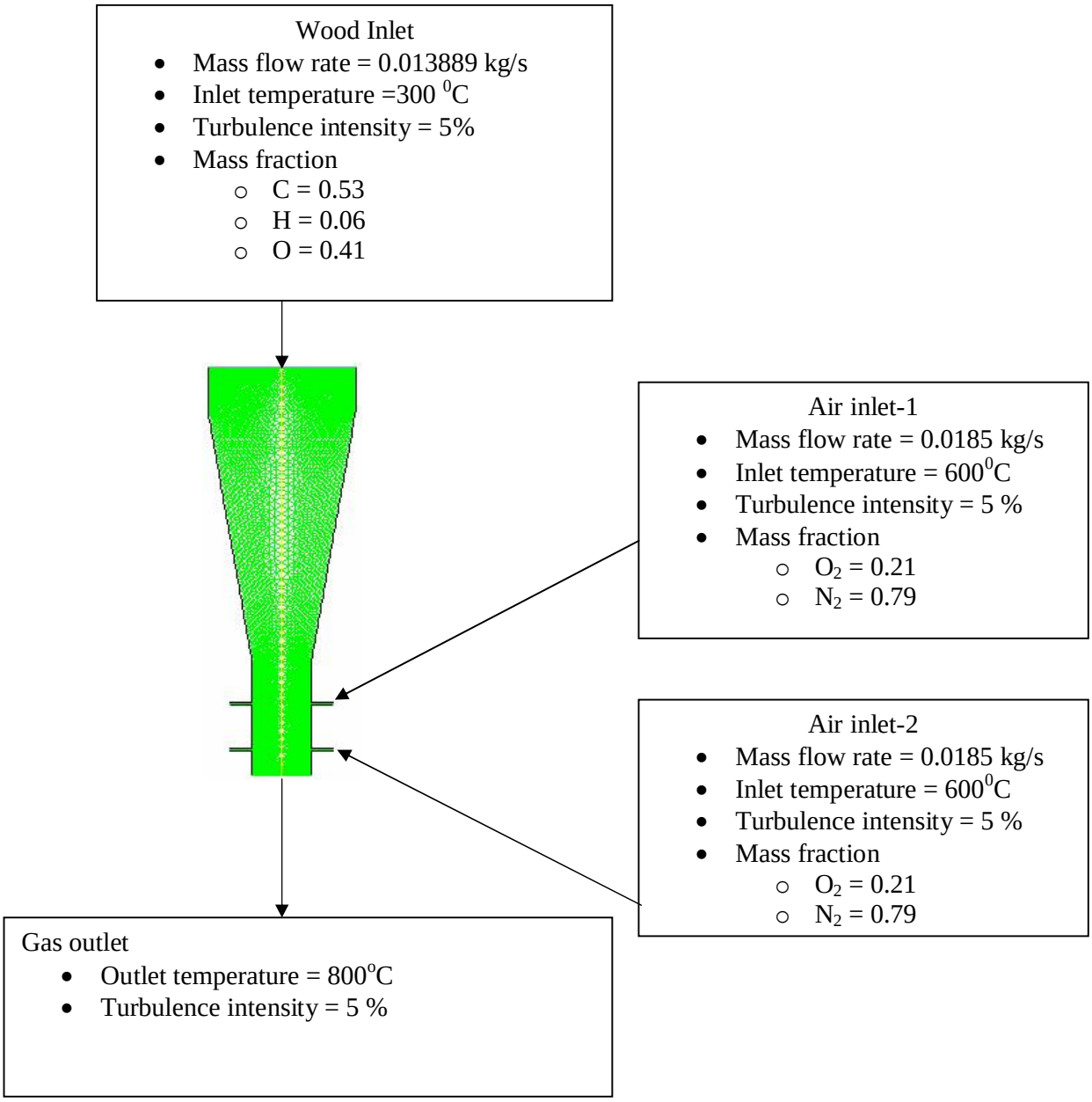

Fig: 3.2 boundary conditions Case 1

erforming the computational simulation are given as follows:

4.1. Pre-processing:

The pre-processing phase starts with the geometry generation. This phase includes geometry generation, mesh generation, fluid properties specifications, physical model selection, and boundary condition specifications.

4.2. Processing:

In the processing phase, the equations and models set up in the pre-processing phase are solved using the CFD code. The progress of the calculation to achieve a converged result is observed. Sometimes adjustments on under-relaxation factors need to be made to help reach the convergence.

4.3. Post processing:

The post processing phase includes the analysis and interpretation of the results. The results can be presented in the form of x-y plots, contour plots, velocity vector plots, streamline plots, and animations.

The pre-processing tool used in this study is GAMBIT, which provides one interface to build and mesh the geometry. The CFD solver is the commercial CFD code FLUENT Version 6.1.22. FLUENT is a finite-volume-based CFD solver written in C language, and has the ability to solve fluid flow, heat transfer and chemical reactions in complex geometries and supports both structured and unstructured mesh. Figure 4.1 illustrates the basic program structure that can be used to support CFD simulation in FLUENT.

The geometry is generated and meshed in GAMBIT. Two-dimensional Triangular mesh is used for meshing the gasifier. A total of 23,316 grids are employed. After the model has been meshed, it is exported to FLUENT.

4.5 Numerical Procedure

The procedure for performing the simulation in FLUENT is outlined below.

1. Create and mesh the geometry model using GAMBIT
2. Import geometry into FLUENT
3. Define the solver model
4. Define the turbulence model
5. Define the species model
6. Define the materials and the chemical reactions
7. Define the boundary conditions
8. Initialize the calculations
9. Iterate/calculate until convergence is achieved.
10. Post-process the results

FLUENT offers two solution methods: (a) segregated solution and (b) coupled solution. Segregated solution solves the governing equations of continuity, momentum, energy, and species transport sequentially (segregated from one another). On the other hand, coupled solution solves the governing equations of continuity, momentum, energy, and species transport simultaneously. The equations for scalars such as turbulence and radiation are solved using the previously updated values from the momentum equations. Segregated solution is chosen for this study. The detailed steps of segregated solution are given below.

(i) Fluid properties are updated based on the current solution or the initialized solution.

(ii) The momentum equations are solved using the current values of pressure and face mass fluxes to get the updated velocity field.

re correction is calculated from the continuity momentum equations since the velocity field obtained in step (ii) may not satisfy the continuity equation.

(iv) The pressure correction equations obtained from step (iii) are solved to correct the pressure and velocity fields, and face mass such that the continuity equation is satisfied.

(v) The equations for scalars such as turbulence, energy, radiation, and species are solved using the updated values of the other variables.

(vi) The equation is checked for convergence.

These steps are repeated until the convergence criteria are met. Figure 4.2 shows the flow chart of the above steps.

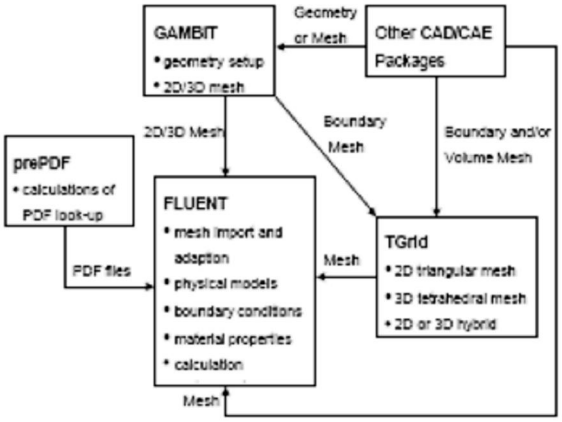

Figure 4.1 Basic program structures

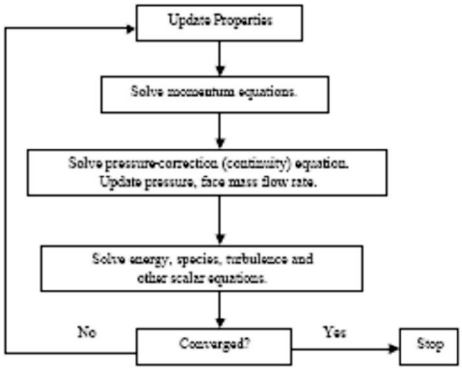

Figure 4.2 Flow chart

equations can be linearized implicitly or explicitly dent variables. If linearized implicitly, the unknown value in each cell is computed using a relation that includes both existing and unknown values from neighboring cells. If linearized explicitly, the unknown value in each cell is computed using a relation that includes only existing values. In the segregated solution, the linearization is implicit. Therefore, each unknown will appear in more than one equation in the linear system, and these equations must be solved simultaneously to give the unknown quantities.

FLUENT uses a control-volume-based technique to convert the governing equations to algebraic equations, which are then solved mathematically. The discretization of the governing equations yields discrete equations that conserve each quantity on a control-volume basis. There are several discretization schemes available in FLUENT: (a) First Order, (b) Second Order, (c) Power Law, and (d) QUICK. The first order discretization scheme is applied for the momentum, the turbulence kinetic energy, the turbulence kinetic dissipation, the energy, and all the species.

FLUENT provides three algorithms for pressure-velocity coupling in the segregated solver: (a) SIMPLE, (b) SIMPLEC, and (c) PISO. The SIMPLE algorithm [Patankar et. al, 1980] is used in this study.

The built-in standard *k-e* turbulence model is used, and the model constants are as follow: $C_m = 0.09$, $C_{1e} = 1.44$, $C_{2e} = 1.92$, $s_k = 1.0$, $s_e = 1.3$.

FLUENT offers several species model: Species transport: laminar finite-rate, eddy-dissipation, or eddy-dissipation concept (EDC)

- Non-premixed combustion
- Premixed combustion
- Partially premixed combustion
- Composition PDF combustion

The species model and transport model with volumetric reaction are chosen to simulate the diffusion and production/destruction of the chemical species. The eddy dissipation model is utilized to calculate the net production and

s. Eddy-dissipation model assumes that chemical o the mixing rate of the reactants by the turbulent fluctuations. A mixture material that consists of seven chemical species (C, O_2, N_2, CO, CO_2, H_2O and H_2) is defined. All the species, including C, are defined as fluid species and are assumed to mix at the molecular level. The specific heat of the species is temperature dependant and is defined as a piecewise-polynomial function of temperature. The chemical reactions (R1.1) through (R1.5) in Chapter 1 are then defined in the reaction window.

The types of boundary conditions on the surface geometry have been assigned inGAMBIT. There are three types of boundary conditions for the model.

1. **Mass flow rate inlet**: All the inlet surfaces are defined as mass flow rate inlets. The mass flow rate, temperature of the mixture, and the mass fractions of all species in the mixture are specified according to the values given in the Table 2.1 in Chapter Two.
2. **Pressure outlet**: The outlet surface is assigned as a pressure outlet boundary. The pressure, temperature, and species mass fractions of the gas mixture outside the computational domain are specified. This information does not affect the calculations inside the computational domain but will be used if backflow occurs at the outlet.
3. **Walls**: The outside surfaces are defined as wall boundary. The walls are stationary with no-slip condition imposed (zero velocity) on the surface. For adiabatic case, the heat flux on the wall is set to 0 (zero). For constant wall temperature, the wall temperature is set to a certain constant value.

The complete inlet and boundary conditions for all the cases conducted in this study are listed in Table 3.1.

Before FLUENT can begin solving governing equations, flow field guessed initial values, used as the initial values of the solution, have to be provided. Once the initial values have been provided, the iteration is performed until a converged result is obtained.

is to model the Biomass gasification process which is considered to be a very complicated process. There are many parameters that affect the efficiency of producer gas production in Biomass gasifiers, such as fuel type, Moisture content in the fuel, equivalence ratio etc. This study of gasification/thermal flow interactions and investigate the effects of these different input parameters on the performance of down draft biomass gasifiers by modelling the gasification process and employing the Computational Fluid Dynamics (CFD) technology would contribute to the industry resolving concerns and improve gasifier efficiency and reliability. The specific goals are:

1. Incorporate the gasification models into a commercial CFD code
2. Simulate a Down draft biomass gasifier
3. Investigate the effects of equivalence ratio over the composition of the producer gas and the calorific value.

Investigation of down draft biomass gasification processes simulation has been carried out with the help of FLUENT, a CFD tool to simulate. The following different operating conditions and parameters on which the study is focussed:

1. Gas outlet temperature
2. Maximum reaction temperature
3. Species mass fraction at the reactor out
4. Calorific value of the gas produced.

The operating conditions and the model parameters used in the simulations for various cases are summarized below. The simulation results on the gas temperature, carbon fuel conversion, and mole fractions of species at the gasifier outlet are discussed in details in the following article.

Calculations:

5.2 Calorific value:

Equivalence ratio (ø) is defined as

$$\phi = \frac{\frac{m_{fuel}}{m_{oxygen}}}{\left(\frac{m_{fuel}}{m_{oxygen}}\right)_{Stoichiomaric}}$$

erage of the species composition for all four obtained from the CFD analysis as an output data. The values for all the our cases as obtained from the cfd analysis is tabled below:

	E 0.20	E 0.25	E 0.30	E 0.35
Mass fraction of H_2	16.78	15.52	20.55	11.11
Mass fraction of CO	19.77	34.01	31.47	19.47
Mass fraction of CO_2	12.86	4.08	5.97	36.65
Mass fraction of CH_4	2.97	0.24	0.18	0.19
Mass fraction of N_2	47.62	46.16	41.83	32.58

Table 5.1 Mass Fraction of components per m^3 of gas produced

These values hence obtained from the analysis are further used for the calorific value of the gas produced. The calculation for the case is as shown in the table below:

Components	**Percentage composition**	**Calorific value**	
		Individual component	**contribution to over all mol wt**
H_2	16.78	12.78	214.45
CO	19.77	12.71	251.28
CO_2	12.86	0	0
CH_4	2.97	39.76	118.01
N2	47.62	0	0
Total calorific of the gas			583.81

Table 5.2 Calorific value calculation table per m^3 of gas produced (Case 1)

.1213/100 = 5.83 Mj/m^3 = 1394.79 k cal/ m^3

dure the calorific value for all the four cases is calculated and the values are tabulated as below:

Equivalence ratio	Calorific value (kcal/m^3 of gas)
0.20	1395
0.25	1529
0.30	1600
0.35	753

Table 5.3 Shows Calorific value for all the four cases

5.3 Gasification efficiency:

Gasification efficiency defined as:

$$\text{Gasification efficiency} = \frac{\text{(Mass of Wood * Calorific value of the wood)}}{\text{(Mass of gas * Calorific value of the gas)}}$$

For case -1 the calculation of gasification efficiency is as given below:

Mass flow rate of wood = 0.013889 Kg/sec

Calorific value of the wood = 4474 Kcal/ kg

Volume flow rate of gas = 2.5 * 0.013889

= 0.034723 m^3/sec

Calorific value of the producer gas = 1388 kcal/m^3

$$\text{There fore gasification efficiency} = \frac{0.013889 * 4474}{0.04723 * 1388}$$

= 77.57 %

on methodology the gasification efficiency is
are presented below in the table

Equivalence ratio	Gasification efficiency (in %)
0.2	80
0.25	85
0.3	89
0.35	42

Table 5.4 shows the gasification efficiencies for all the four cases

biomass gasifier has been carried out with help of FLUENT, a CFD tool to simulate the effect of equivalence ratio on the product gas composition. The Down draft gasifier considered under this study is a 100 kg/hr wood gasifier with constant wood consumption at varied air flow conditions. The product gas composition is studied with different equivalence ratios as 0.2, 0.25, 0.3 and 0.35. It is assumed that the gas hence produced is exhausted to the atmosphere so the pressure at exit of the gasifier is assumed to be atmospheric. Analysis gives the effect of equivalence ratio on producer gas composition, calorific value and maximum reaction temperature.

.

The following conclusions can be drawn from the results:

6.1. Fig 6.1, 6.9, 6.16, 6.23 shows the contours generated by FLUENT. These figures indicate that the temperature gradient along the height of the reactor for different equivalence ratios. Further it is noticed that for all the cases the maximum temperature are at the nozzles and a temperature gradient exists along the height of the reactor.

6.2. Further it is evident from the temperature gradient that formation of different zones along the height of the reactor with reference to the temperature at that particular zone.

6.3. The top most portion of the reactor i.e. hopper where the temperature is varying from atmospheric to 100^{o}C is the drying zone. In the drying zone the moisture present in the wood evaporates.

6.4. Further just below the drying where the temperature is in the band of 200 to 600 is the distillation zone where the volatile matter present in the wood evaporates. Further in this model volatile matters are not considered for the analysis.

6.5. The position where the air is injected is the oxidation where the seven reactions discussed in the chapter 2 takes place. Further the gasifier under study being a down draft gasifier hence the concentration of the Species are higher at the bottom portion of the reactor.

6.6. Fig 6.8, 6.15, 6.22, 6.29 (contours) shows the velocity profile of the air injected into the reactor for gasification for four different equivalence

s at the air inlet points are maximum for all the four

6.7. Fig 6.6, 6.14, 6.21, 6.28 (contours) shows the variation in mass fraction of C(s) for all the four cases. Further these figures indicate the a clear trend that as the equivalence ratio is increased the mass fraction of C(s) decreases to negligible quantity at the bottom portion This is because of more air availability all the Carbon present in the wood reacts with O2 in the air to form CO, and CO_2.

6.8. Fig 6.2, 6.10, 6.17, 6.24 (contours) shows the variation in mass fraction of H_2 for all the four cases. Further it is noticed that the H_2 Mass fraction at the outlet of the gasifier for ER 0.3 is maximum value of 20%. Further it also noticed that the beyond ER 0.3 it reduces drastically to 11% at ER 0.35.

6.9. Fig 6.4, 6.11, 6.18, 6.25 (contours) shows the variation in mass fraction of CH_4 for all the four cases. Further it is noticed that the CH_4 Mass fraction at the outlet of the gasifier for ER 0.2 is maximum value of 3%. Further it also noticed that the beyond ER 0.2 it reduces drastically to 0.24 at ER 0.25 and remains constant at that value even the ER is increased.

6.10. Fig 6.5, 6.12, 6.19, 6.26 (contours) shows the variation in mass fraction of CO for all the four cases. Further it is noticed that the CO Mass fraction at the outlet of the gasifier for ER 0.25 is maximum value of 34%. Further it also noticed that the beyond ER 0.25 CO Mass fraction reduces.

6.11. Fig 6.4, 6.11, 6.18, 6.25(contours) shows the variation in mass fraction of CO_2 for all the four cases. Further it is noticed that the CO_2 Mass fraction at the outlet of the gasifier for ER 0.35 is maximum value of 37%. Further it also noticed that the minimum value occurs at ER 0.25 of 4%.

6.12. It is noticed from the above graph that the maximum calorific value is obtained at equivalence ratio 0.30 which is1600kCal/m3 of gas. It is noticeable that the calorific value increases as the equivalence ratio increases from 0.2 to 0.25 and further increase in the equivalence ratio the trend reverses and the calorific value reduces with increase in

lence it is advisable to operate the gasifier at an f below ø = 0.3 or just at ø = 0.30 to obtain maximum calorific value of the producer.

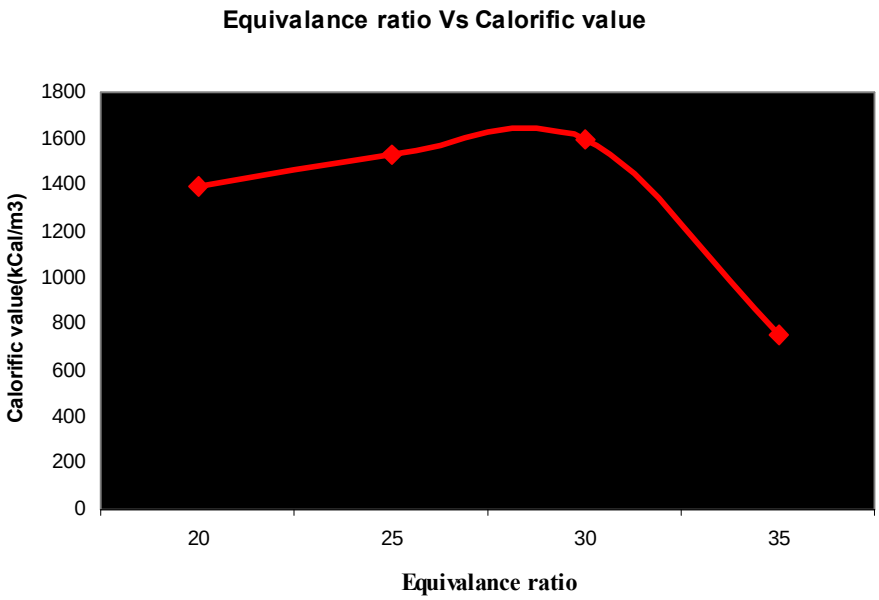

6.13. Similarly the Gasification efficiency at different equivalence ratio is calculated and presented in the form of the graph shown above. Further it is evident from the above graph the efficiency is maximum at equivalence ratio 0.30. Hence equivalence ratio 0.30 is the best suitable condition for gasification since at this equivalence ratio both the gasification efficiency and the calorific is maximum.

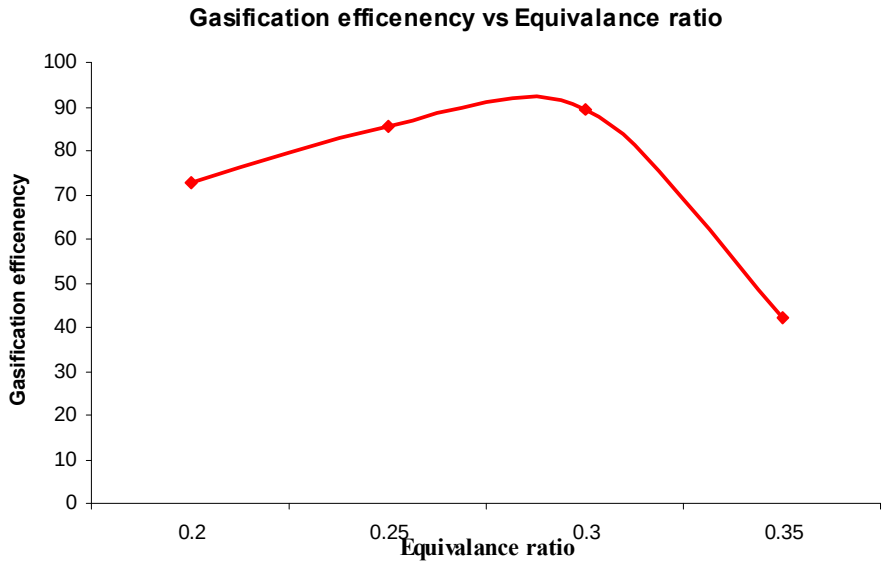

ion temperature reported below is the temperature the reactor. The outcome of the analysis is that the maximum reaction temperature increases as the equivalence ration increases. As the equivalence ratio increase the partial combustion processes converts into complete combustion and hence it is noticeable that the temperature shoots up significantly as the equivalence increases beyond 0.3.

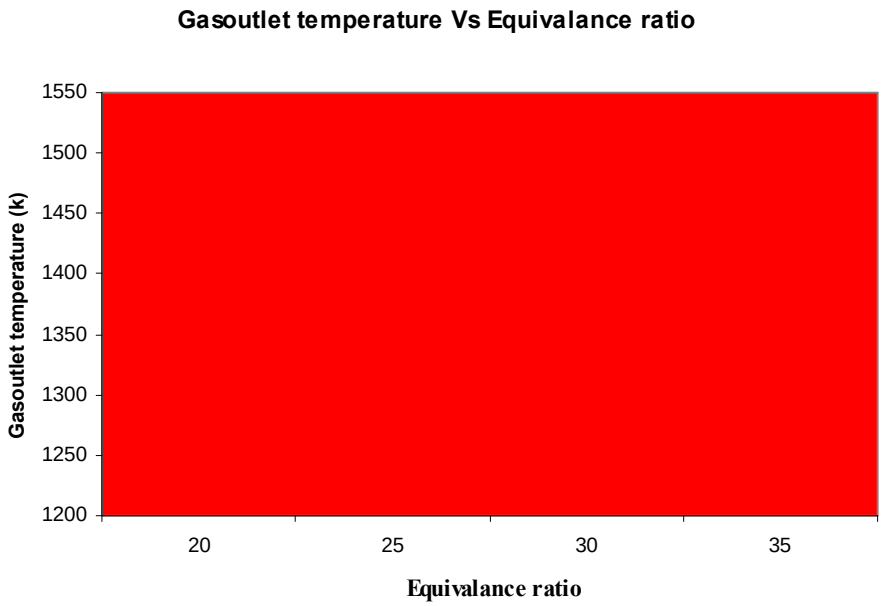

NS FOR FUTURE WORK CHAPTER 7

The current project enabled the basic understanding and formulation of 2d models for study of the gasification using CFD code. However more detailed models are required for extending these models to achieve results which can be applied into practical situations. The following list of possibilities is present for future work on this subject:

- Study of tar and tar modelling in a gasifier
- Construction of steady state models for pyrolysis and gasification zones.
- Comprehensive modeling of a gasifier in which the various models developed can be combined to obtain realistic results.
- Formulation of a design procedure for construction of a biomass gasifier and pyrolyzer on the basis of the above models.

le, February 2003.

[2] Thomas B. Reed and Agua Das Hand book of biomass downdraft gasifier engine systems SERI SP-271-3022 DE 88001135 March1998.

[3] Patankar S.V., Numerical Heat Transfer and Fluid Flow, McGraw Hill, 1980.

[4] Iyer, P. V. R., Rao, T. R., Groover, P. D., Singh, N. P., 2002, ñBiomassï Thermochemical Characterization,ò Chemical Engineering Department, Indian Institute of Technology, Delhi, pp. 9 ï 16.

[5]Z.A.Zainal,AliRifau,G.A.Quadir,K.N.Seetharamu. Experimental investigation of a downdraft biomass gasifier.biomass and bioenergy 23 (2002) 283-289

[6] Reed, T., Markson, M., 1983, ñA Predictive Model for Stratified Downdraft Gasification of Biomass,ò In Proc. Of the Fifteenth Biomass Thermo chemical Conversion Contactors Meeting, Atlanta, GA, pp. 217-254.

[7] Dasappa, S., Paul, P. J., Mukunda, H. S., 2000, ñGasification Theory and Design-Renewable Energy for Rural Areas,ò Indian Institute of Science, Bangalore

[8] Bridgwater, A. V., 1995, ñThe Technical and Economic Feasibility of Biomass Gasification for Power Generation,ò Fuel, Vol. 74, pp. 631-653.

[9] Reed TB, Das A.Handbook of biomass downdraft gasifier engine system. Golden, CO: SERI, 1988

[10] Bridgwater, A. V., ñThe Technical and Economic Feasibility of Biomass Gasification for Power Generation,ò Fuel, 1995; Vol. 74, pp. 631-653.

[11] Bhattacharya, S. C., Hla, S. S., Pham, H. L., 2001, ñA Study on a Multistage Hybrid Gasifiers-Engine System,ò Biomass and Bioenergy, Vol. 21, pp. 445-460.

[12] Vriesman, P., Heginuz, E., Sjostrom, K., 2000, ñBiomass Gasification in a Laboratory- Scale AFBG: Influence of the location of the Feeding Point on the Fuel-N Conversion,ò Fuel, Vol. 79, pp. 1371-1378.

[13] P.P.Parikh,A.G.Bhave,D.V.Kapse&Shashikantha, Study of Thermal and Emission Performance of Small Gasifier-Dual-Fuel Engine Systems, Biomass 19 (1989) 75-97.

[14] Gen Gas, 1982, Tipi Workshop Publications.

[15] S. Gaur & T.B. Reed, ñA survey of biomass gasification.ò

[16] D.L. Giltrap, R. McKibbin & G.R.G. Barnesa , òA steady state model of gas-char reactions in a downdraft biomass gasifier.ò

oeters, ñModeling of biomass gasificationò

, ñBiomass Gasifier ñTarsò: Their Nature, Formation, and Conversion.ò

[19] Belleville & Capart, ñA model for predicting outlet gas concentrations from a wood gasifier.ò

[207] W.F. Degroot & F. Shafizadeh, ñKinetics of wood gasification by Carbon Dioxide and steam.ò

[21] C. Franco, F. Pinto, I. Gulyurtlu & I. Cabrita, ñThe study of reactions influencing the biomass steam gasification process.ò

[22] B. V. Babu & P.N. Sheth, ñModeling and simulation of biomass gasifier: effect of oxygen enrichment and steam to air ratio.ò

[23] T.H. Jayah, ñComputer simulation of a downdraft wood gasifier for tea drying.ò

[24] G.M. Simmons & W.H. Lee, ñKinetics of gas formation from cellulose and wood pyrolysis.ò

[25] M.S. Sundaram, Meyers Stemberg & Peter T. Fallon, ñFlash pyrolysis of biomass with reactive and no-reactive gases.ò

[26] F. Shafizadeh, ñPyrolytic reaction and paths of biomass.ò

[27] R.K. Jalan, V.K. Srivastava, ñStudies on pyrolysis of a single biomass cylindrical pellet kinetic and heat transfer effects.ò

[28] A.S. Chaurasia & B.V. Babu, ñModeling and simulation of pyrolysis of biomass: effect of thermal conductivity, reactor temperature and particle size on product concentration ranges.ò

[29] K.M. Bryden & M.J. Hagge, ñModeling the combined impact of moisture and char shrinkage on the pyrolysis of a biomass particle.ò

[30] Babu, B. V., & Chaurasia, A. S., ñPyrolysis of Biomass: Improved Models for Simultaneous Kinetics and Transport of Heat, Mass, and Momentumò

[31] B.V. Babu & A.S. Chaurasia, ñModeling, simulation and estimation of optimum parameters in pyrolysis of biomass.ò

[32] M. Syamlal, W. Rogers & T. J. O'Brien, ñMFIX Documentationò

[33] Mechanical Wood Products Branch, FAO Forestry Department,ò Wood gas as engine fuel.ò

[34] A.V. Bridgewater, G.L.Ferrero & K. Manitias, òCommercial and marketing aspects of gasifiers.ò

Case 1 ER 0.20

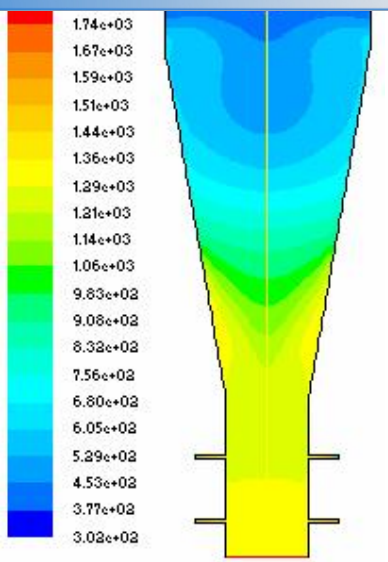

Fig 6.1 Case 1 Temperature profile contours

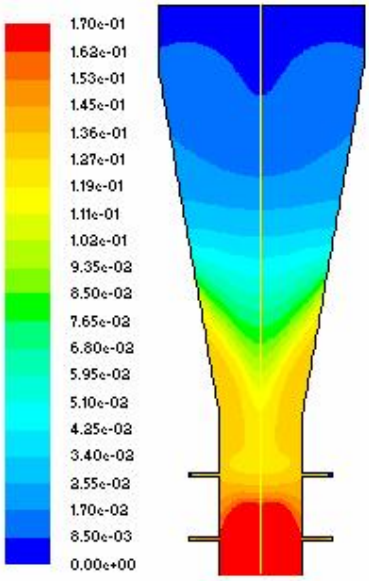

Fig 6.2 Case 1 Mass fraction h_2 contours

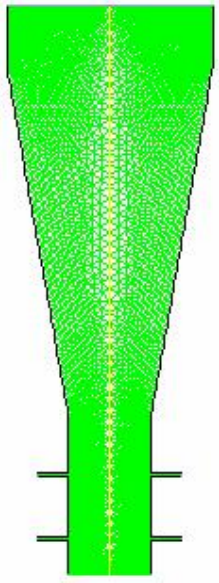

Fig 6.3 Case 1 Grid

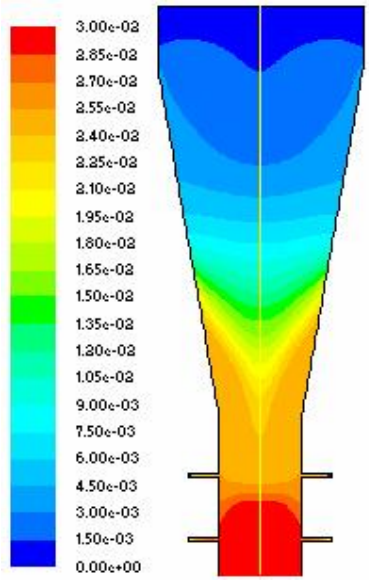

Fig 6.4 Case 1 Mass fraction Ch_4 contours

Case 1 ER 0.20

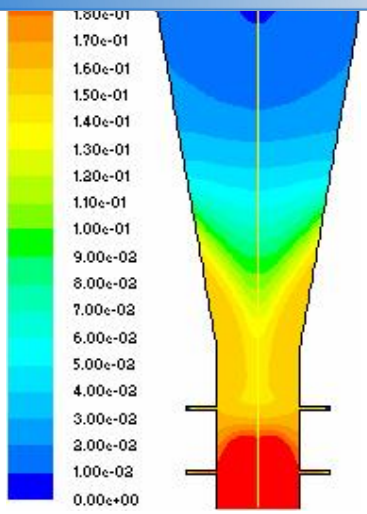

Fig 6.5 Case 1 Mass fraction CO contours

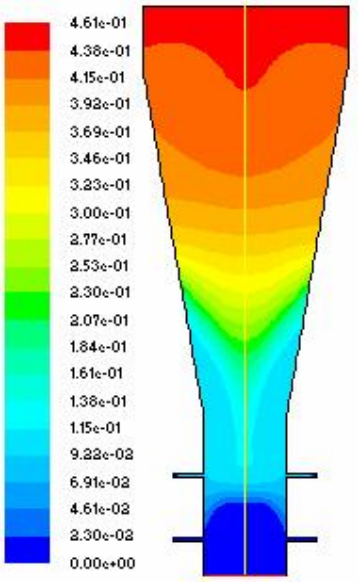

Fig 6.6 Case 1 Mass fraction C(s) contours

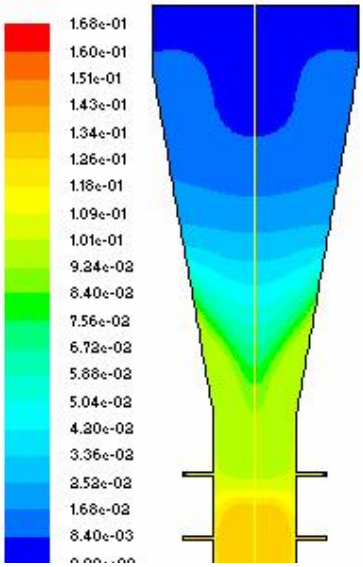

Fig 6.7 Case 1 Mass fraction CO_2 contours

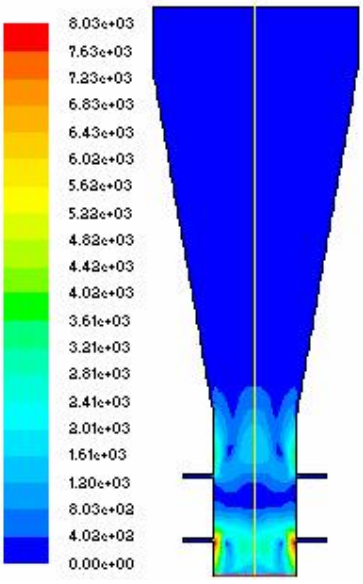

Fig 6.8 Case 1 Velocity contours

Case 2 ER 0.25

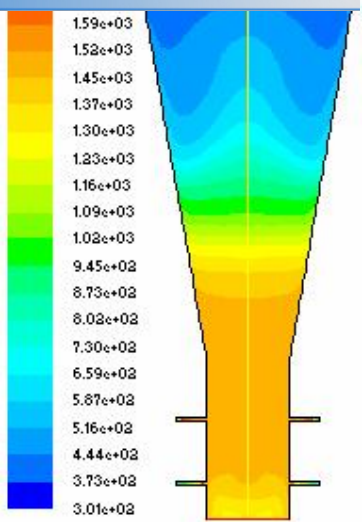

Fig 6.9 Case 2 Temperature profile contours

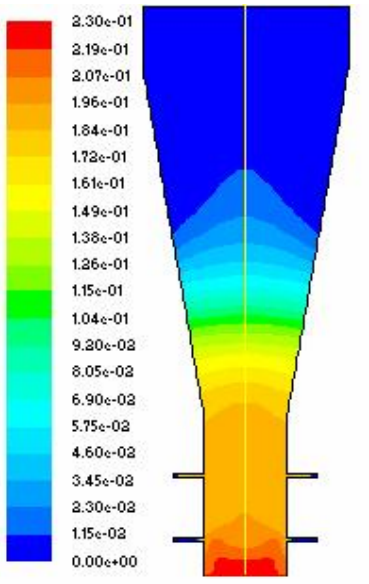

Fig 6.10 Case 2 Mass fraction h_2 contours

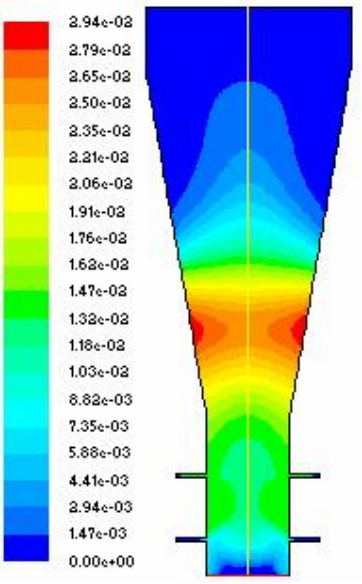

Fig 6.11 Case 2 Mass fraction Ch_4 contours

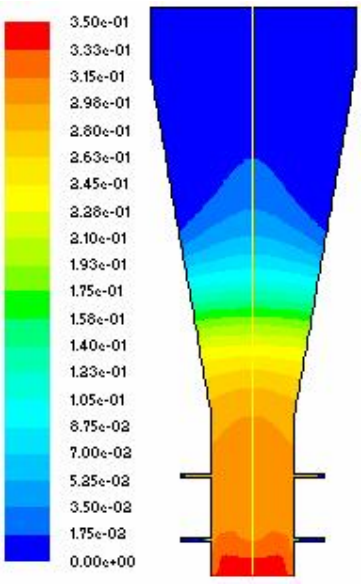

Fig 6.12 Case 2 Mass fraction CO contours

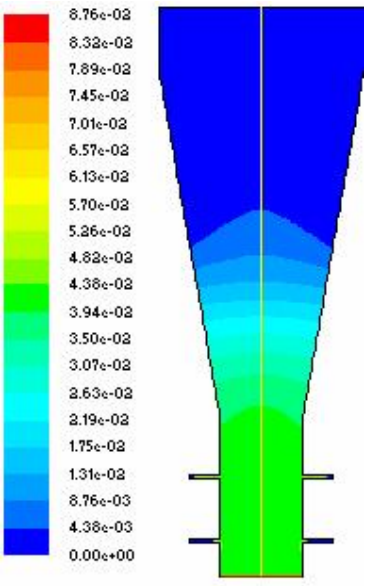

Fig 6.13 Case 2 Mass fraction CO_2 contours

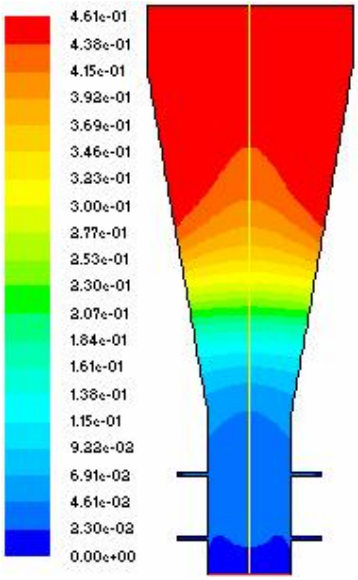

Fig 6.14 Case 2 Mass fraction C(s) contours

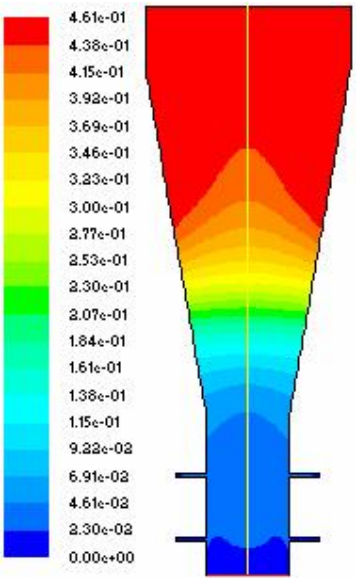

Fig 6.15 Case 2 Velocity contours

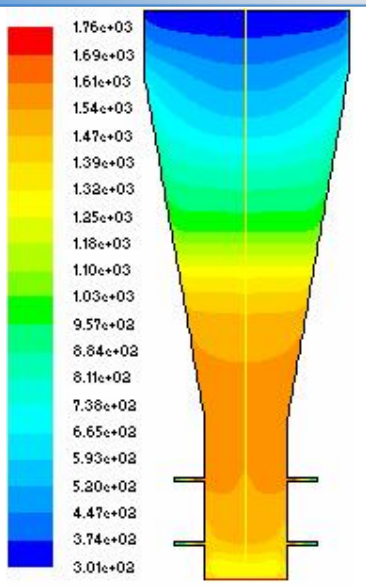

Fig 6.16 Case 3 Temperature profile contours

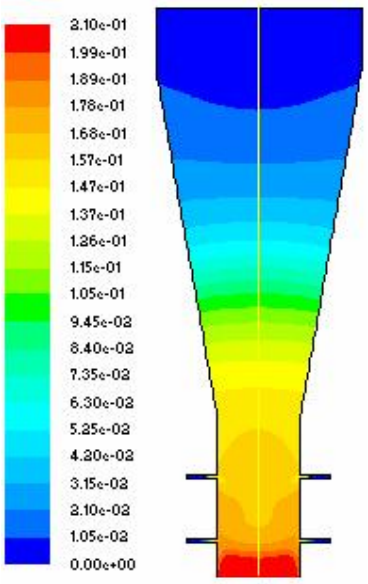

Fig 6.17 Case 3 Mass fraction h_2 contours

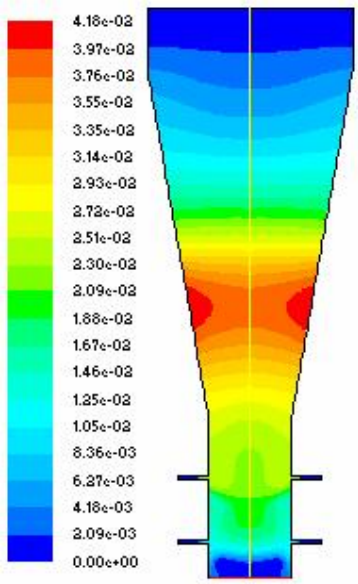

Fig 6.18 Case 3 Mass fraction Ch_4 contours

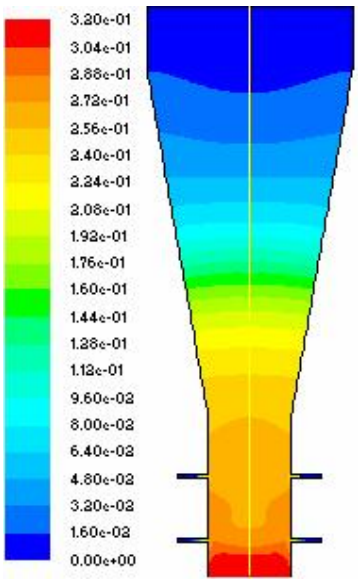

Fig 6.19 Case 3 Mass fraction CO contours

Case 3 ER 0.30

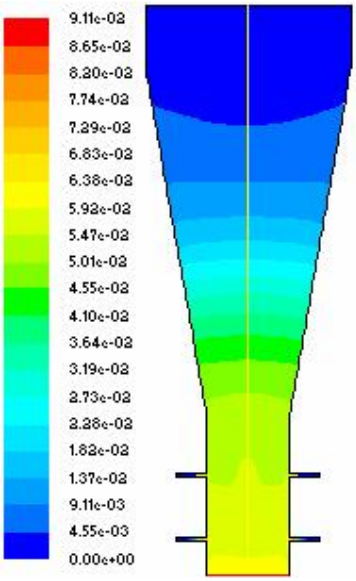

Fig 6.20 Case 3 Mass fraction CO_2 contours

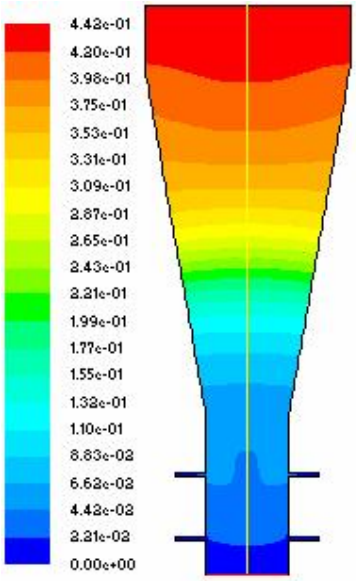

Fig 6.21 Case 3 Mass fraction C(s) contours

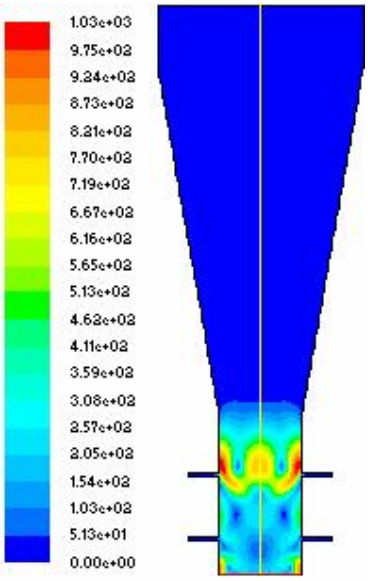

Fig 6.22 Case 3 Velocity contours

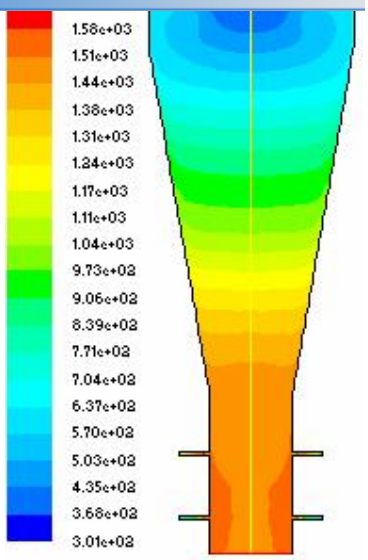

Fig 6.23 Case 4 Temperature profile contours

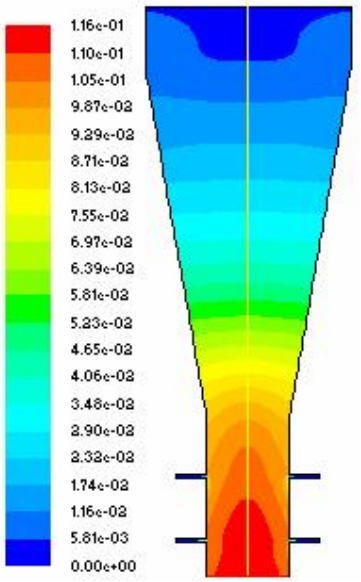

Fig 6.24 Case 4 Mass fraction h_2 contours

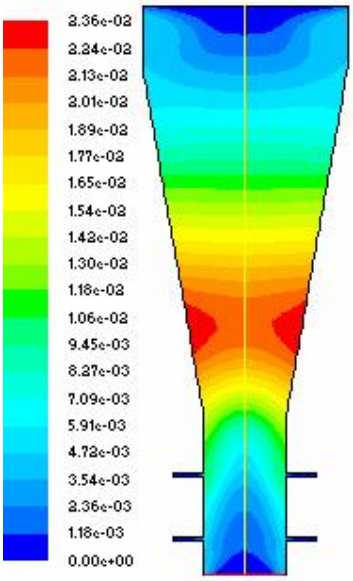

Fig 6.25 Case 4 Mass fraction Ch_4 contours

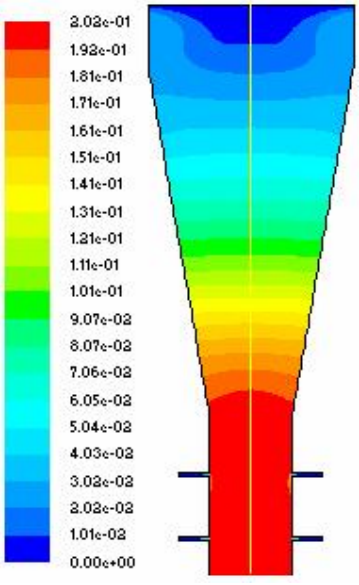

Fig 6.26 Case 4 Mass fraction CO contours

Case 4 ER 0.35

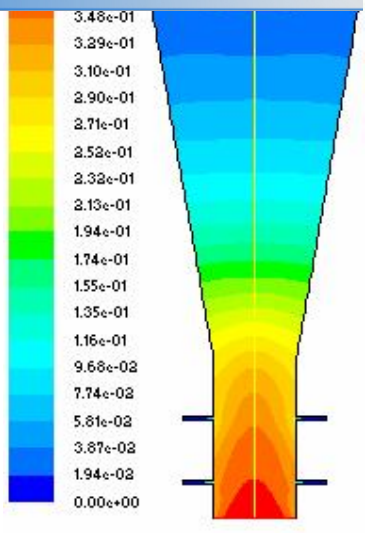

Fig 6.27 Case 4 Mass fraction CO_2 contours

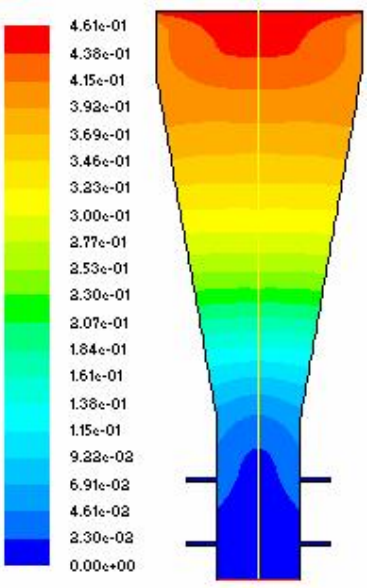

Fig 6.28 Case 4 Mass fraction C(s) contours

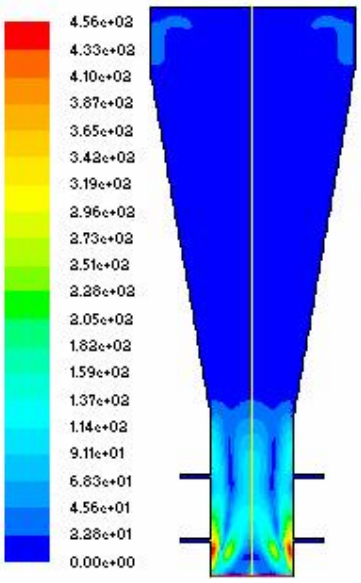

Fig 6.29 Case 4 Velocity contours

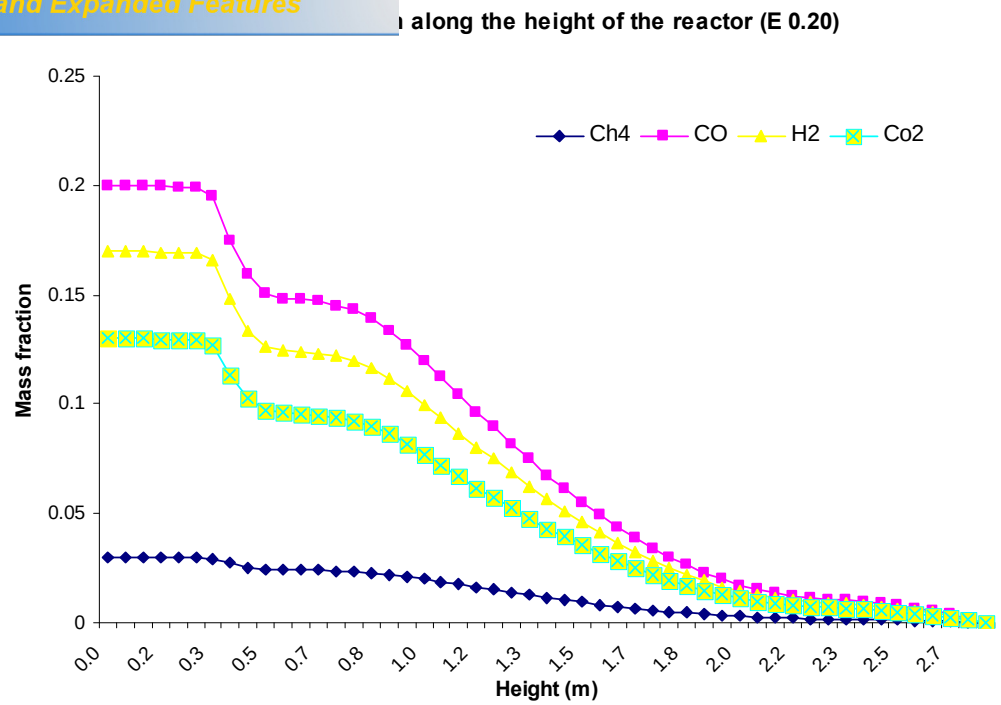

Fig 6.30 Mass fraction of Species (E0.20)

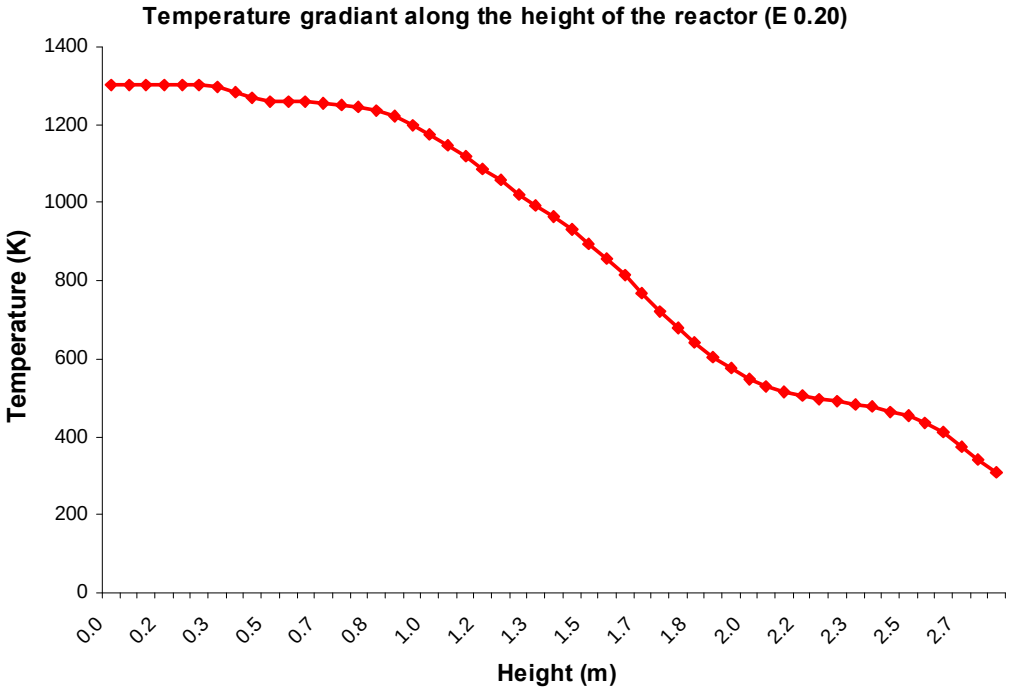

Fig 6.31 Temperature gradient (E 0.20)

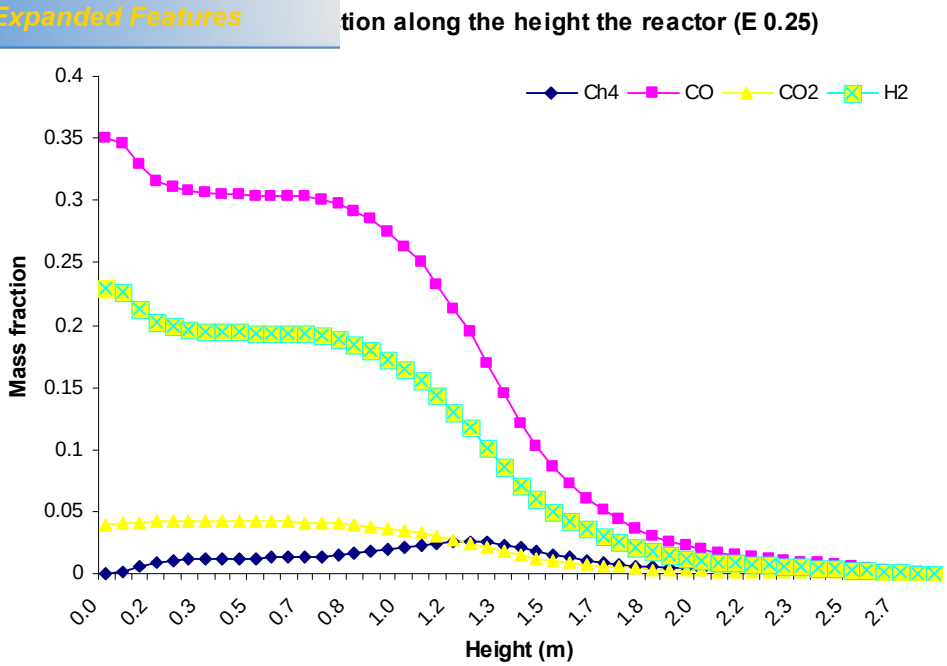

Fig 6.32 Mass fraction of Species (E0.25)

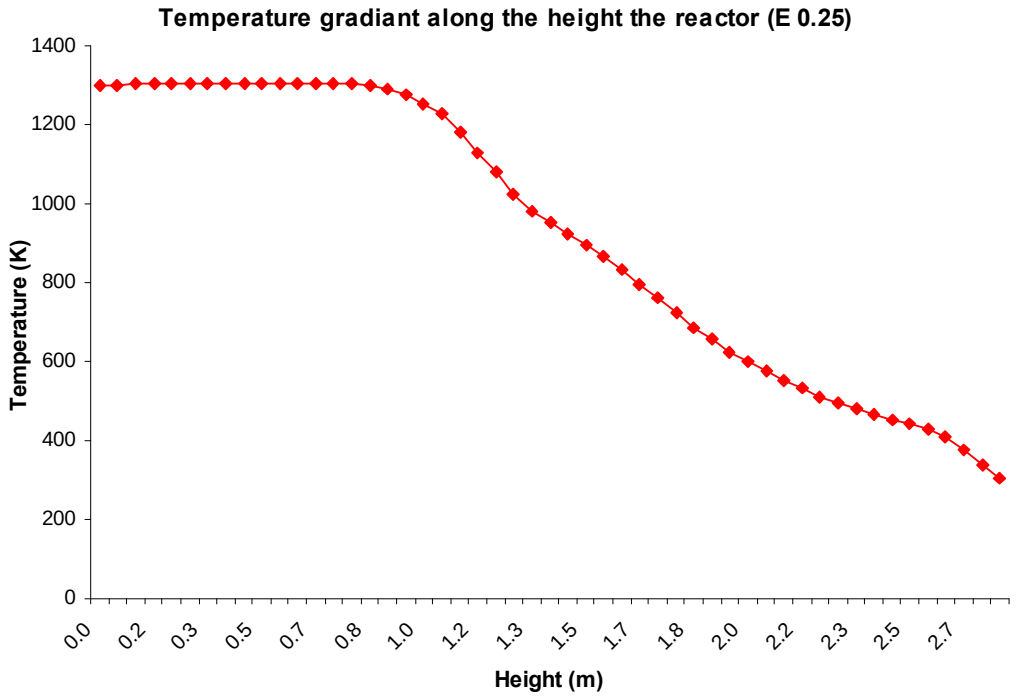

Fig 6.33 Temperature gradient (E 0.25)

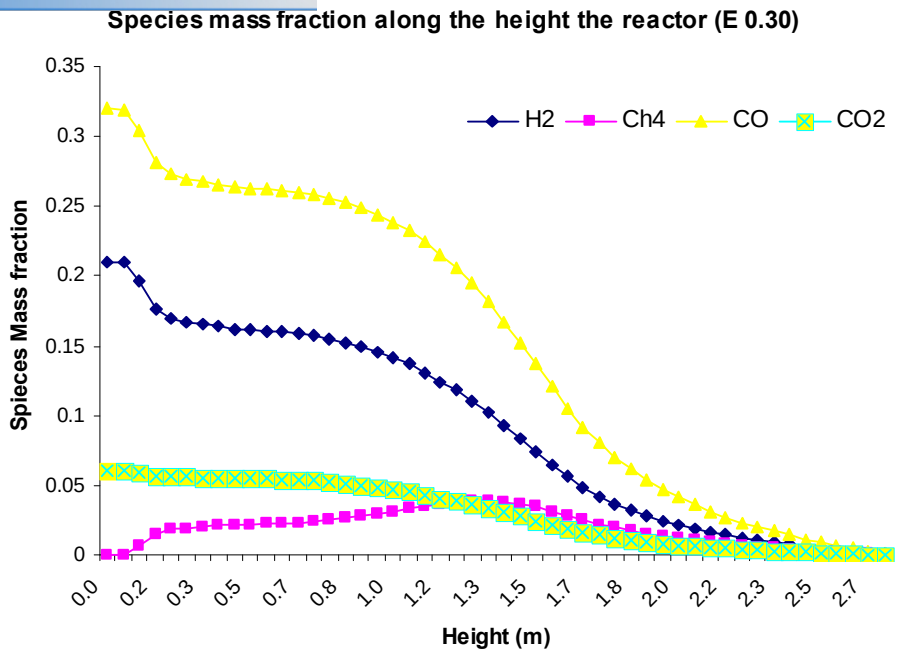

Fig 6.34 Mass fraction of Species (E 0.30)

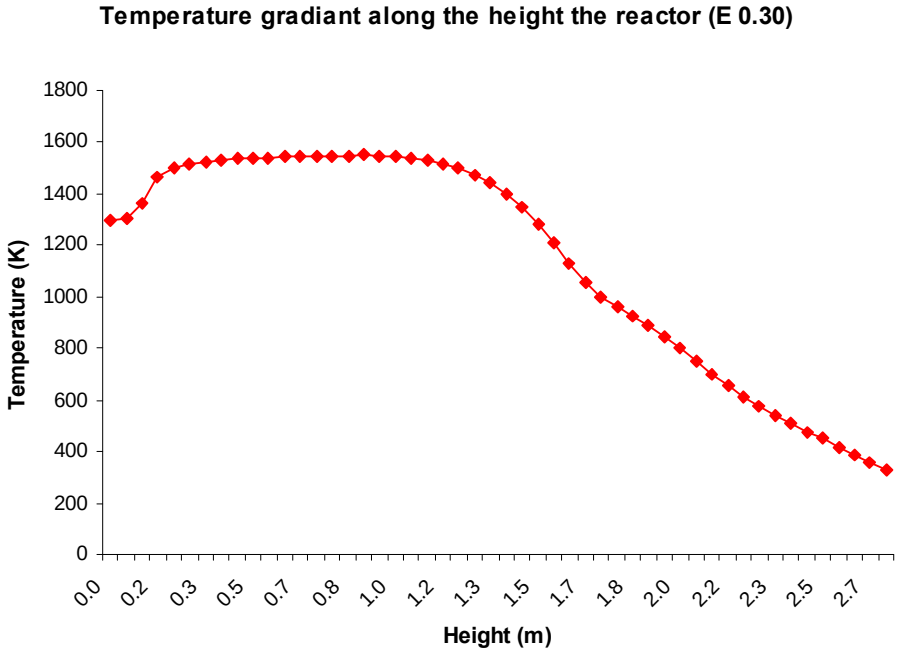

Fig 6.35 Temperature gradient (E 0.30)

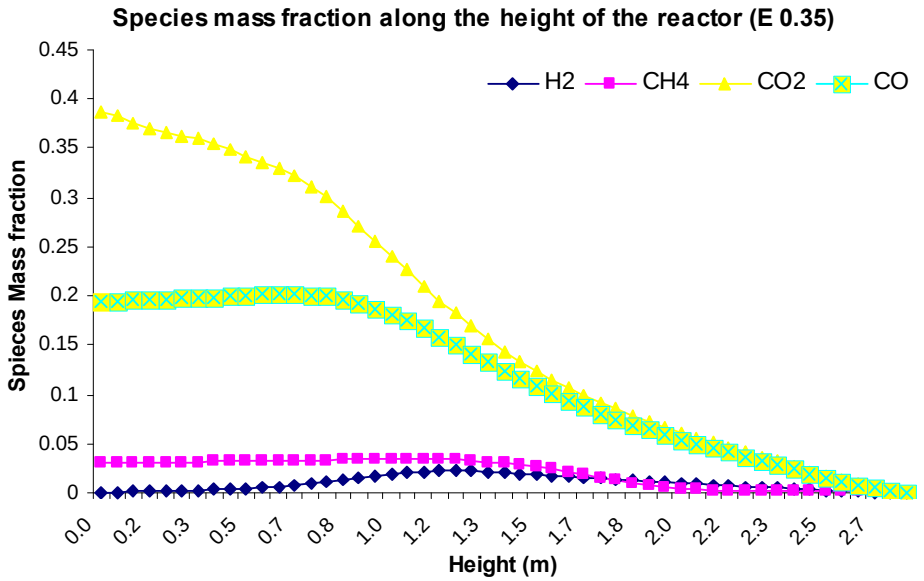

Fig 6.36 Mass fraction of species (E 0.35)

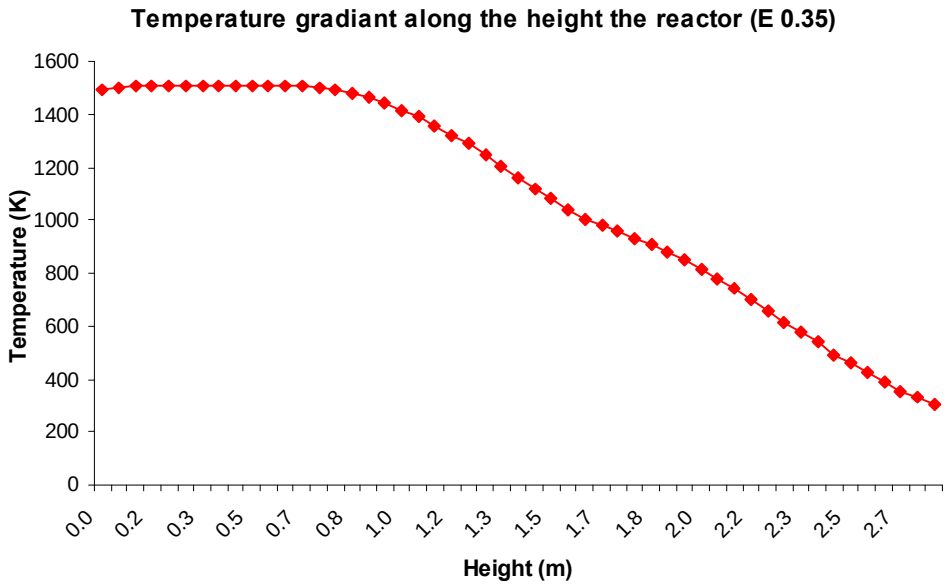

Fig 6.37 Temperature gradient (E 0.35)

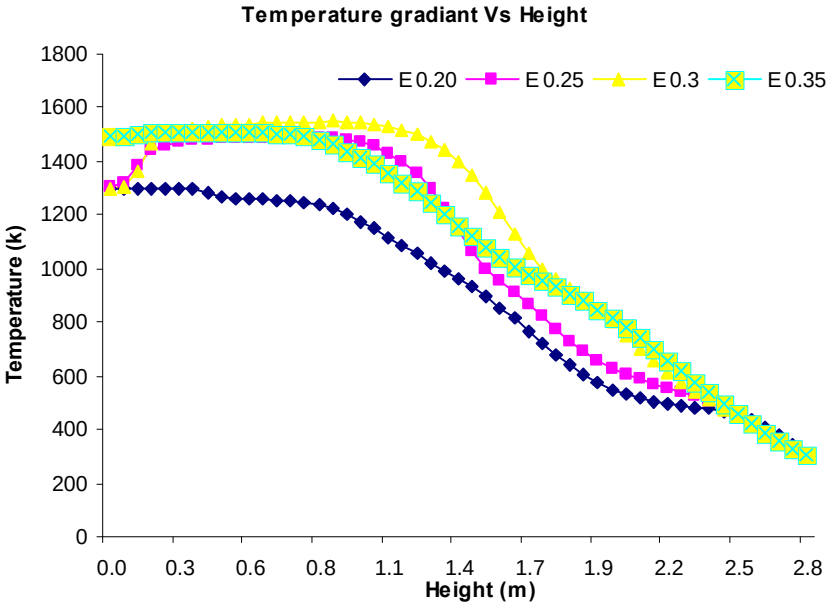

Fig 6.38 Comparison of Variation in Temperature gradient

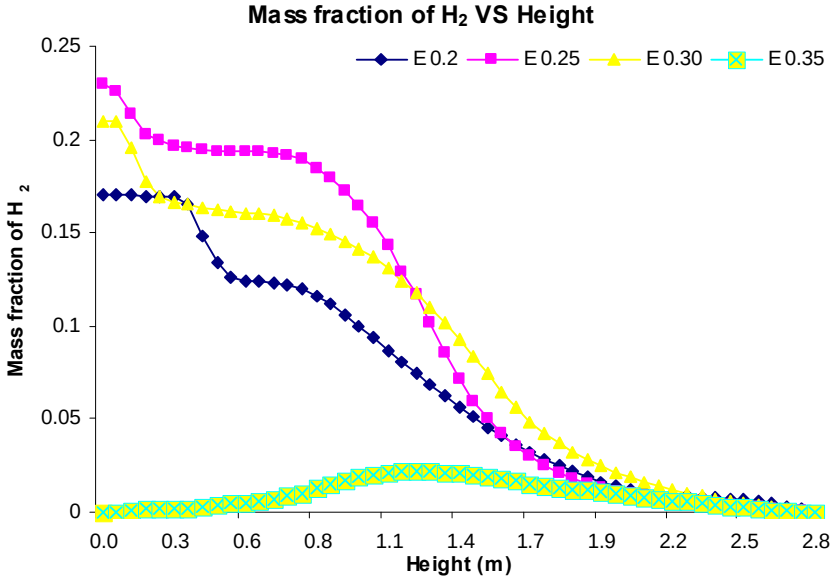

Fig 6.39 Comparison of Variation in mass fraction of H_2

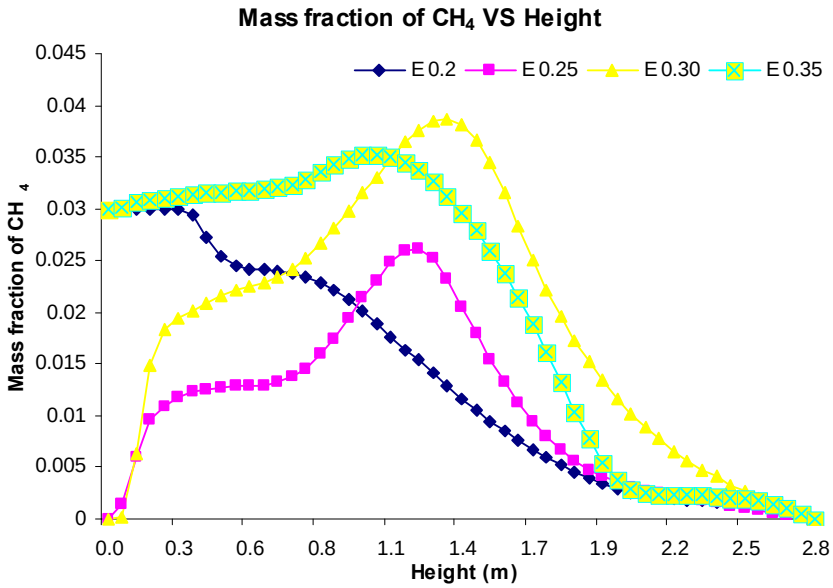

Fig 6.40 Comparison of Variation mass fraction of CH_4

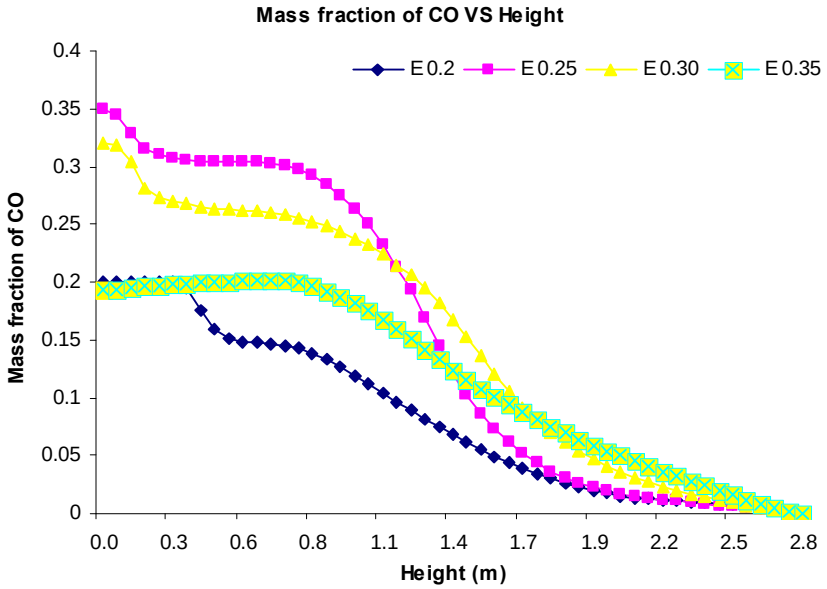

Fig 6.41 Comparison of Variation mass fraction of CO

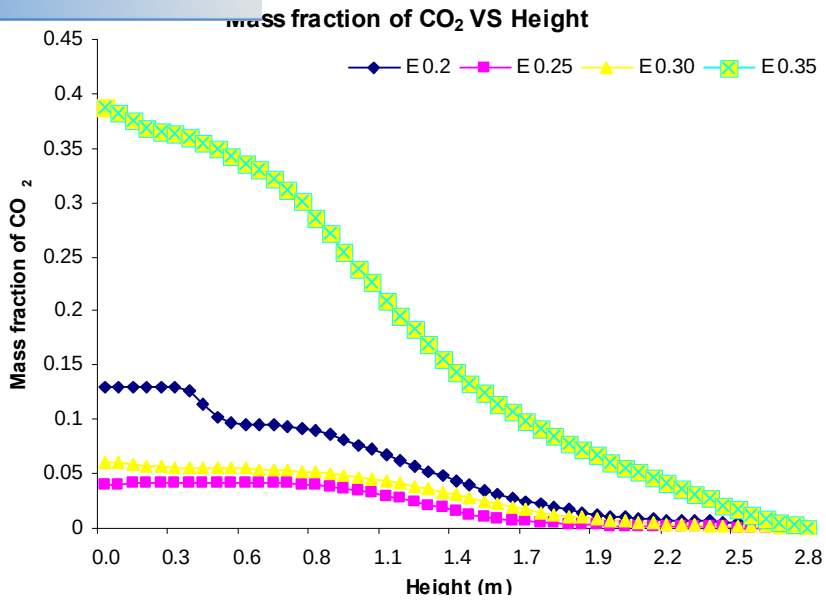

Fig 6.42 Comparison of Variation mass fraction of CO_2

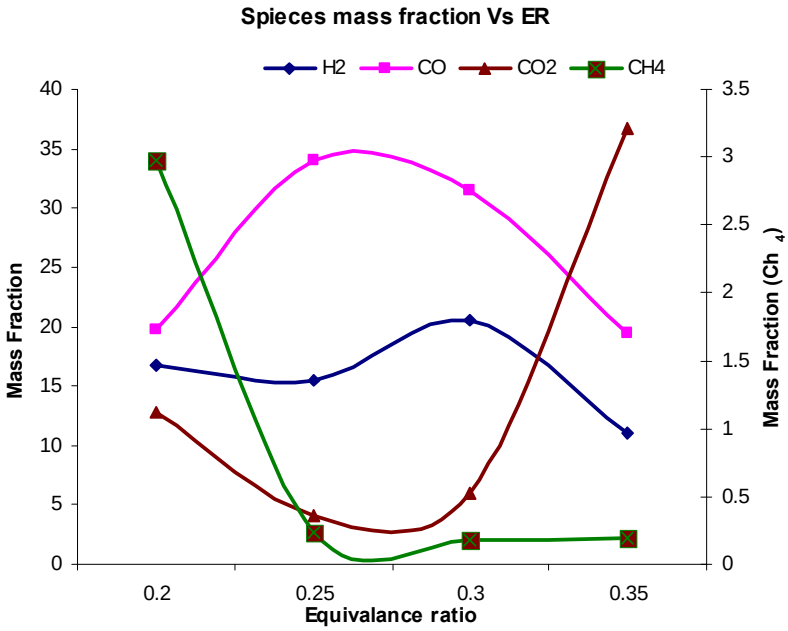

Fig 6.43 Comparison of Variation mass fraction Species